HELLENIC REPUBLIC
National and Kapodistrian University of Athens
EST. 1837

"ALEXANDER FLEMING"
Biomedical Sciences Research Center

REGENERON
SCIENCE TO MEDICINE

«In vitro μικροφυσιολογικά συστήματα για φαρμακολογικές μελέτες σε ανθρώπινα γαστρεντερικά οργανοειδή»

«In vitro microphysiological systems for pharmacological studies on human gastrointestinal organoids»

M.Sc. Dissertation Thesis

International MSc in Molecular Biomedicine: Mechanisms of Disease, Molecular and Cellular Therapies and Bioinnovation

Medical School, National and Kapodistrian University of Athens and BSRC "Alexander Fleming"

ANGELOS MICHAILIDIS

Thesis Supervisor
Dr. Katia Catherine Karalis, Executive Director, Regeneron Pharmaceuticals, Inc.

Committee Members
Prof. Maria Tsoumakidou, Associate Professor, Medical School of Athens
Prof. George Kollias, Professor, Medical School of Athens

ATHENS 2024

PROLOGUE

The current study was performed at the Regeneron Pharmaceuticals Tarrytown Campus in the United States of America, under the supervision of Dr. Katia Catherine Karalis.

First of all, I would like to thank Dr. Karalis for her constant support and mentorship throughout this year.

Furthermore. I would like to thank Dr. Manasvi Shah for her guidance and continuous support with both theoretical and practical knowledge, which were pivotal to the completion of this study.

Last but not least, I would like to thank Alexandros Kokkosis, Elias Pavlopoulos, Esraa Ismail, Kristen Howell, Sarah Neuner and Shek Man (Jacky) Chim for their flawless collaboration and for providing a pleasant and educational work environment.

Contents

PROLOGUE 2

Abstract 4

1. Introduction 5

1.1 Models of healthy and diseased tissue 5
1.1.1 Limitations of conventional models of disease 5
1.1.2 Organoids 6

1.2 Microphysiological systems 8
1.2.1 Basic principles 8
1.2.2 Human Organoids-on-Chip 9

1.3 Colorectal Cancer 11
1.3.1 General Characteristics 11
1.3.2 Disease progression 12

1.4 Modeling the intestine on a chip 14
1.4.1 Conventional models of the gut 14
1.4.2 Novel ways of culture for better in vivo/in vitro relevance 15

2. Aim of the study 18

3. Materials and Methods 19

3.1 Organoid Culture 19
3.1.1 CRC Organoids 19
3.1.2 Colon Organoids 20

3.2 Establishment of Organoids-on-chip systems 22
3.2.1 Culture Protocol 22
3.2.2 Proinflammatory Cytokines and Seeding of PBMCs 25
3.2.3 Culture and recruitment of PBMCs 26
3.2.4 Barrier function analysis 26

3.3 Immunofluorescence staining 27
3.3.1 Immunostaining of Colon Organoids-on-Chip 27
3.3.2 Immunostaining of CRC Organoids-on-Chip 28
3.3.3 Immunofluorescence Reagents 30

3.4 Quantification of proinflammatory cytokines on chip effluents 31

4. Results 32

4.1 Establishment and characterization of Colon-on-chip 32

4.2 Modeling of immune cell recruitment in the context of TNF-α induced inflammation. 35
4.2.1 Increased permeability of the intestinal barrier 39
4.2.2 Verifying PBMC activation 39

4.3 Establishment of CRC organoids 40

4.4 Establishment and evaluation of CRC-on-a-Chip 41
4.4.1 Resistance of CRC lines to intestinal barrier disruption 47

5. Summary 48

References 50

Abstract

The intestine is a complex organ with a variety of functions that are significant for organismal health and it stands as a well-studied tissue in the field of biomedicine, since it is liable to a variety of pathologies, that pose a great burden to society. Although numerous in vivo models have been developed to study gastrointestinal diseases, the intricate processes associated with human physiology and pathogenesis are not easily translated to animal models and hence the majority of clinical trials end up in failure. In this study, we employed human derived intestinal organoids in combination with organ-on-chip platforms, in order to develop humanized models of colon health and disease. We successfully recreated a colonic tissue on a chip, with differentiated epithelial cells, a developed endothelial compartment, and a robust intestinal barrier that was disturbed under an inflammatory setting. Furthermore, we designed a model of peripheral blood mononuclear cells (PBMC) recruitment, emulating the in vivo migration of these cells to the site of inflammation. This model aimed to provide a humanized and physiologically relevant platform to evaluate the efficacy of immune cell-dependent therapeutic proteins in development for the treatment of colorectal cancer (CRC). Thus, we established patient derived CRC organoid lines with different phenotypes and mutational background, which were then seeded on chips under identical conditions. CRC organoids developed morphologically distinct tissues and the integrity of the intestinal epithelial barrier remained undisturbed after exposure to interferon-gamma (IFN-γ), possibly hinting to the resistance of the pathology towards proinflammatory stimuli. Although the molecular mechanisms underlying our observations are subject to further investigation, we were successful at designing models of human relevant health and disease, which hold significant potential for advancing drug discovery.

1. Introduction

1.1 Models of healthy and diseased tissue

1.1.1 Limitations of conventional models of disease.

Animal models and traditional two-dimensional (2D) cell cultures have long been the basis of all biomedical studies, giving rise to groundbreaking insights on the molecular mechanisms governing human biology. However, there are plenty of caveats using these models to study human physiology due to the absence of the natural tissue microenvironment or the lack of relevancy to the human cell-cell interactions. While conventional 2D monolayer cell cultures are much less demanding to use and maintenance than any other biological model, they are unable to fully recapitulate the characteristics of a tissue in an in vivo state, due to the absence of the proper architecture, adhesion forces and environmental cues [1]. In the context of cancer, 2D cell lines have a significantly different molecular profile in comparison to human tumors [2], making them a far less representative disease model than an in vivo tissue. The relative clinical relevance of findings based on immortalized 2D cell lines is partly due to the accumulating genomic instability and the phenotypic differences between each passage [3], but also due structural and phenotypic variation [4]. While short-lived, primary cell lines have greater clinical relevance than immortalized ones, they still can't reproduce the cellular heterogeneity within a tumor or recapitulate the tumor immune microenvironment, both of which are aspects of utmost importance in the biology and evolution of cancer, and thus, in the context of immunotherapy [2,5]. Additionally, cells in 2D cultures are forced to grow in a monolayer with apicobasal polarity and in the absence of an extracellular matrix, therefore their growing conditions can be considered somehow artificial and hence, they have restricted clinical and biological relevance as a cellular model to reflect on systemic responses, even when they are incorporated in co-cultures or transwell systems [6]. Small animal models are also a staple tool in biomedical research, since they have led to important discoveries on understanding the biological mechanisms governing diseases and they are used to evaluate the pharmacokinetic properties, efficacy and safety of novel therapeutics before testing on humans [7]. However, the actual success in the translation of animal data to human is limited, due to unforeseen and often severe toxicities or lack of efficacy that were not picked up by the preclinical studies [7,8]. For example, in clinical cancer trials the success rate for the accurate translation between animal models and humans has been reported as lower than 10% [7]. Additionally, animal models have a non-human microenvironment and thus a completely different innate immune response which could play a prominent role when modeling diseases such as cancer or inflammatory diseases. An additional caveat is that animal models can usually capture parts of the disease progress or the host immune response, such as in cancer xenografts, for example [2]. All in all, conventional models to study physiology and disease progress have played a vital role in advancing our knowledge on the molecular mechanisms governing life and the development of innovative therapies, while they also bear significant limitations for drug

discovery, with the higher success rate observed in monogenic diseases where mouse and human genetic causes and the associated pathways overlap.

1.1.2 Organoids

Organoids are three-dimensional (3D) in vitro cellular systems, derived from differentiation of induced pluripotent stem cells (iPSCs) or primary, tissue derived progenitor cells. Organoids emulate significant aspects of in vivo organ functional and micro-anatomical properties [9,10]. Multiple tissue cell types are usually represented in a single organoid, that are self-organized through spatially restricted lineage commitment, hence they can accurately recapitulate the tissue-specific developmental programs [1]. Late advancements in stem cell technology have been crucial for the field, particularly after the landmark study of Sato and Clevers in 2009, in which they demonstrated the development of self-organized intestinal epithelial structures, composed of multiple cell-types and reminiscing of the originating organ, from just a single, Lgr5^{+}, intestinal stem cell [9,11]. Organoids can be generated using embryonic stem cells (ESCs), but also patient derived pluripotent stem cells (PSCs) and organ-specific adult stem cells (ASCs) [12], providing a great potential for applications in human disease modeling, patient cohorts stratification and precision medicine, drug discovery and ultimately, regenerative medicine [13] (**Figure 1**).

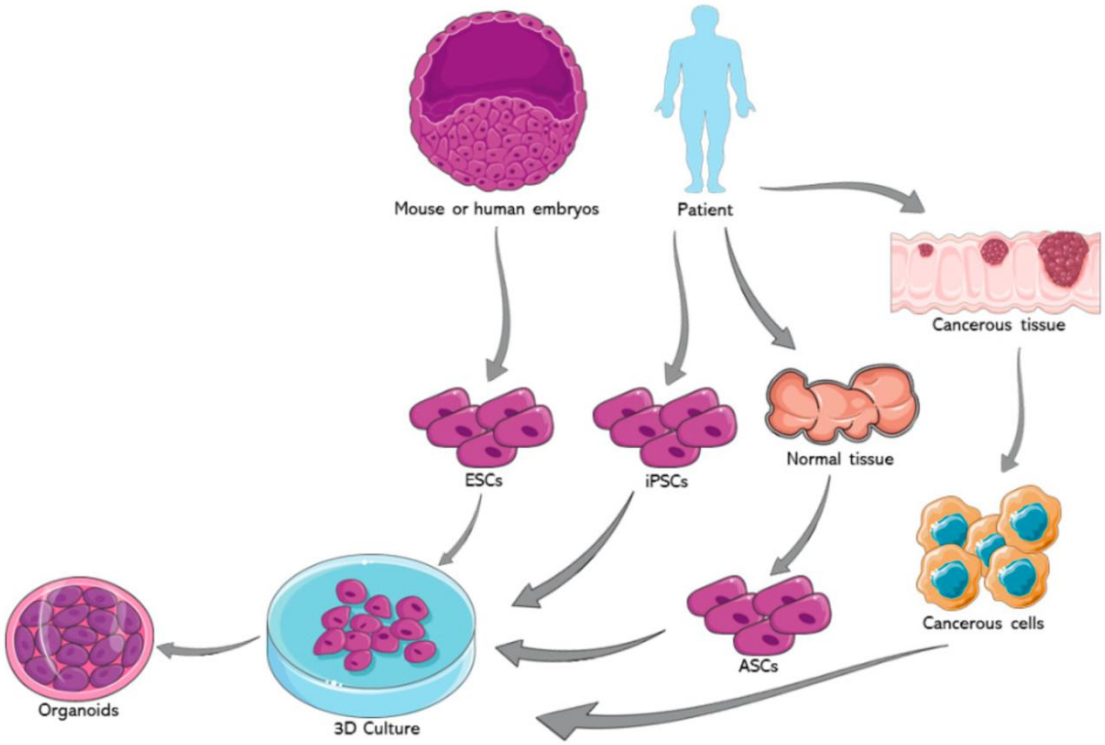

Figure 1. Generation of organoids from different types of stem cells. **Azar et al. International Journal of Molecular Sciences 2021.**

Organoids and in general the multicellular systems, can provide human-specific, accurate systems to elucidate, and even model, cell-cell interactions in normal and disease states. In order to reconstruct informative tissue/organ models, it is essential to reconstruct, to the extent it is feasible, the environmental cues that drive the fate and function of each cell type (**Figure 2**). A critical component of the tissue microenvironment is the extracellular matrix (ECM), which provides support for the development and 3D self-organization of cells in culture. One of the most commonly used ECM-like materials in that context is Matrigel, a mix of ECM components, cytokines, transcription factors and growth factors [14,15]. Matrigel is an extract of Engelbreth–Holm–Swarm mouse sarcomas, which acts as a basement-membrane matrix that has been shown critical in supporting the growth, self-organization and differentiation of many different cell types and thus, it is widely used in organoid generation, propagation and maintenance [13,16]. However, its actual composition is highly variable as shown at the proteomic, biochemical and structural level [10,14]; hence, several alternatives with better characterized compositions can be used to overcome Matrigel's limitations, such as other biological synthetic, or recombinant matrices [10,14,17]. Among the most widely tested are synthetic hydrogels, like polyethylene glycol (PEG) and its derivatives, that have tunable biomechanical properties and a perfectly characterized chemical composition. However, naturally derived matrices, despite their batch-to-batch variability, offer peak biophysical properties, and cell-interacting epitopes that support the development and differentiation of cells, in a more in vivo-relevant manner [18]. Recently, matrices with predefined shapes, engineered through laser cutting, 3D printing or micromanufacturing, are used to provide physical boundaries that will facilitate establishment of a tissue architecture, more similar to the one in an in vivo state [9,19]. Another element crucial to engineering the niche for the maturation of organoids, similar to other tissue-specific multicellular systems, besides the specific ECM composition, is the incorporation of physical cues that guide morphogenesis, such as soluble factors, including growth factors or small molecules, which regulate cell signaling [10].

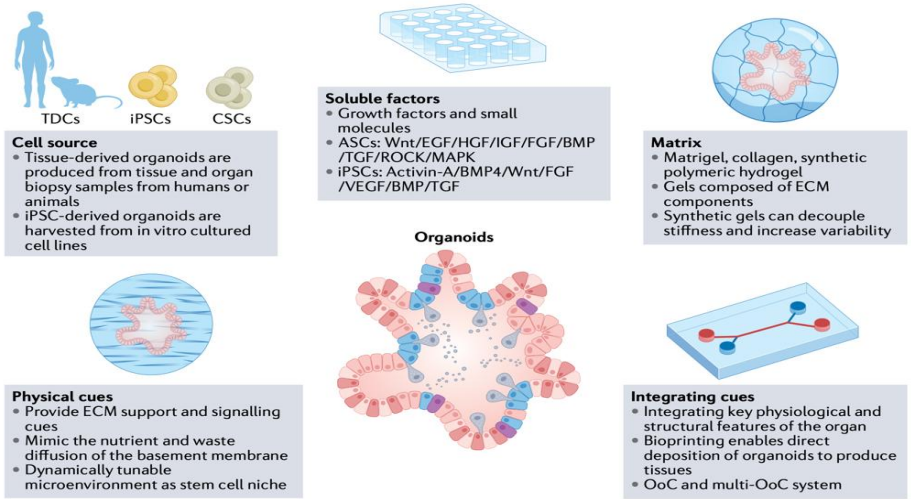

Figure 2. Engineering the organoid niche. **Zhao et al. Nature Reviews Methods Primer 2022.**

There are many advantages in using organoids instead of other traditional models like animal models and 2D cell lines. First of all, organoids mimic key architectural and functional aspects of in vivo tissues [20] and they can include multiple cell lines, derived from distinct germ layers [21]. These characteristics cause significant changes in the phenotype of the cells within an organoid, conferring greater similarity of expression profiles between organoids and in vivo tissues than with monolayered cultures [22,23], thus making them an ideal tool in the context of personalized medicine, by accurately predict drug responses at an individual patient-specific level [24]. In addition, they can theoretically be maintained in cultures indefinitely, retaining their phenotypic and genetic identity, unlike primary cells which have a finite lifespan and may eventually undergo senescence or dedifferentiation [25–27]. Unfortunately, though, organoids have some significant limitations in recreating a tissue, such as the lack of vascularization which could impede their growth and maturation, as well as the presence of high heterogeneity amongst tissue-derived organoids. [1] Specifically, organoids always form a typical conformation, that although it contains multiple cell types and can usually provide insights in different developmental stages, they lack the specific tissue architecture. Additionally, depending on their derived tissues, organoids may fail to fully mature beyond a certain developmental stage, such as retinal and cerebral organoids, in which the full maturation of photoreceptors and cortical plate layers respectively are unable to form at a full capacity [1]. On the contrary, intestinal organoids are capable of producing certain characteristics of a mature phenotype, and capture pathology associated with some genetic defects such as CFTR mutations, as far as these are not dependent on the final tissue architecture or topology-specific cell-cell interactions [28]. Not to be downplayed, the functionality of several organoids has been demonstrated in vivo, following transplantation performed in mice [29–31]. The latter serves as a prototype for tissue regeneration or for “rescuing” in cases of genetic mutations driving critical disease development. Overall and despite certain caveats in the use of organoids to recapitulate organ development and physiology, they represent a dynamic model, with the potential to be a critical asset in cell therapies, disease understanding, human clinical trials and drug development.

1.2 Microphysiological systems

1.2.1 Basic principles

In order for cells to behave as if they were in their native milieu, it is crucial that their complex microenvironment be reconstructed. Microphysiological systems (MPS) are complex and physiologically relevant multicellular organ models, based in the design of a microenvironment that fosters cell-cell interactions similar to those in vivo, enabling organ functions representative of health and disease [18]. The innovative feature of MPS is that they leverage tissue engineering technologies to mimic the natural microenvironment through the control of physical, biochemical, electrical, mechanical and

structural parameters and incorporate challenges associated with diseased tissue states [18]. MPS can accommodate cells from a variety of sources, such as primary cells, organoids, cancer cells, cell explants and induced pluripotent stem cells (iPSCs) in a single model [32,33] tissue-specific, or even -derived, ECM that provides both physical and chemical cues for the maturation and overall functionality of the cells [34]. There are multiple examples illustrating this term, such as organoids, engineered micropatterned tissue constructs, trans-well cultures, and lately, organ-chips, which represent the pinnacle of all MPS, hence they have often become synonymous to the MPS term. In these innovative platforms, engineering and biomimicry collide to capture the in vivo physical and functional architectures of human tissues, with increased control over multiple parameters, making them a more physiologically or even human relevant alternative model to study physiology and disease, with minimal ethical concerns and more accurate in vivo predictions for drug safety and efficacy in a patient-specific manner.

1.2.2 Human Organoids-on-Chip

Organoids-on-Chip is a new experimental platform that was developed in an effort to overcome the limitations of organoids and maximize their potential in biomedical research. The chips are made of poly-dimethylsiloxane, a polymeric rubber like material that is transparent, allowing real time imaging analysis of tissue responses to environmental stress [33], and they usually contain at least two chambers coated by a matrix and separated by a porous membrane, allowing studies on how two different tissues interact [33,35], or providing mechanistic insights on cell migration through these interfaces [36], while at the same time offering independent control over various parameters and the microenvironment of each tissue[37]. The most essential feature of organs-on-a-chip are the microfluidic properties that they offer, which allow a dynamic control of the cellular microenvironment through a continuous nutrients supply and waste removal, but also through the establishment of biochemical gradients. This feature is also responsible for the recreation of the mechanical forces that cells would face in a continuous flow of body fluids, and it also allows modeling of various physiological aspects, such as the interaction of tissue with circulating blood cells and the recreation of a vascular system or a tissue barrier, in combination with a porous membrane [33]. Although the most basic components of a microfluidic device are their channels and chambers, they may also comprise micropumps and valves, which provide additional control over fluid flow, but also electrodes and sensors to monitor in real time parameters like pH, oxygen levels, pressure, temperature, transepithelial/transendothelial electrical resistance (TEER), electrical conduction, biomarker levels and the overall tissue function [18,33]. Additionally, organ-on-chips can incorporate mechanical stimuli like stretching [36] or hydraulic compression [38] and even apply electrical signals [39] that can further mimic the dynamic events experienced by cells and result in a more effective tissue differentiation and clinical relevance. The combination of organoids with organs-on-chip platforms takes advantage of the 3D self-organization and differentiation of organoids with the dynamic regulation of the physiologically relevant microenvironment of a chip [40]. Self-organized primary or stem cell derived human organoids undergo natural differentiation

and display a higher degree of complexity and physiological relevance [41], allowing the study of differentiation and developmental processes that occur naturally in vivo. Additionally, the use of patient derived organoids that contain their unique mutational background opens up the opportunity to study personalized responses to drugs, characterize genetic disorders and understand genetic diversity. Organoids on their own however can only replicate a spectrum of the entire organ structure and physiology and they present an extensive batch to batch heterogeneity. Additionally, they are unable to interact with other organoids, or tissues, a critical caveat for their maturation and morphogenesis. Their incorporation in chips allows the creation of advanced organ models with improved function, complexity and reproducibility. The chip setting allows better control of biophysical cues, such as stretching, topological structure, and stiffness of the substrate and biochemical cues, like growth factor gradient, in the microenvironment (**Figure 3**) and therefore it allows a dynamic regulation of organ development, resembling the natural in vivo cues [40]. Shear stress caused by fluidic flaw is a fundamental mechanical stimulus for proper development and a major advantage of chips. Kidney organoids grown on steady cultures cannot fully mature and develop limited vascularity, even though extensive vascular network is necessary for core kidney functions, however when grown under flow they exhibit enhanced vascularity and more mature phenotype, based on gene expression profiles and the extensive morphogenesis of tubular epithelium [42]. Likewise, brain organoids display enhanced neural differentiation, cortical organization and expression of cortical layer markers when cultivated on a chip with a 3D matrix and continuous fluid flow, allowing the study of developmental processes that are not possible in a static culture [43]. An intestine-on-chip platform with peristalsis-like motions through cyclic suctions has been shown to facilitate the formation of villi-like projections in a duodenal organoid, along with differentiation to multiple intestinal cell types that are crucial for in vivo gut physiological function, while also exhibiting basic intestinal functions like nutrient absorption and mucus production were confirmed with sufficient reproducibility [44]. The expression profile of organoids-on-chip was also compared to the ones in vivo, but also against plain organoid cultures, established intestinal cell lines and organ-on-chips that were made using intestinal cell lines, showing that the organoids-on-chip was the model with the highest relevance towards the in vivo setting [44]. Another emerging application of organoid-on-chips is the ability to combine organoids, derived from multiple tissues, to model multi-organ interactions, an essential aspect of organ development [40]. In that context, an organ-on-chip device containing heart and liver organoids has been used to assess hepatic-dependent cardiotoxicity, under the administration of antidepressant drugs [45]. Lastly, organoids-on-chips can be to assess the interactions between organoids and commensal microbiota or resident immune cells, shedding light on unknown host-immune and host-microbiota interactions and their effect on development, disease and drug response, while concurrently they are also accessible to analytical flux, such as biochemic and electrophysiological analyses, which can be tedious or limited on conventional organoids, impeding their translational applications [40].

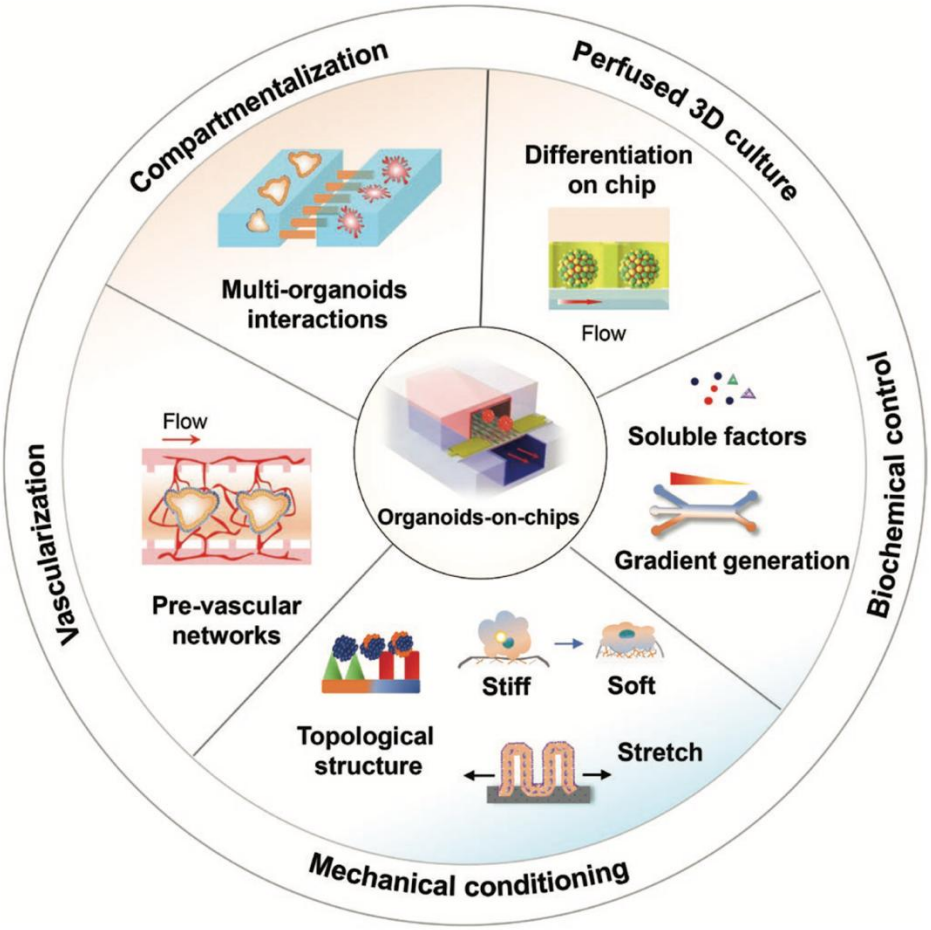

Figure 3. Novelties of the Organoids-on-chip platforms. **Wang and Qin. Life Medicine 2023.**

1.3 Colorectal Cancer

1.3.1 General Characteristics

Colorectal Cancer (CRC) is a neoplastic disease characterized by great heterogeneity and severe metastatic lethality. It is the second and third most diagnosed cancer in women and men respectively and one of the leading causes of cancer-related deaths [46–48]. The epidemiology of the disease differs across countries, however the highest prevalence is observed in developed countries, mostly due to elements of the western lifestyle including obesity, lack of exercise, smoking, age, genetic/hereditary predisposition and environmental factors (**Figure 4**). Symptoms of the disease include abdominal pain, anemia, change in bowel habits and rectal bleeding, however CRC is mostly asymptomatic until the advanced stages of the disease, except rectal bleeding which is common in both malignant and early-stage benign cases [46]. The clinical outcome of the disease is heavily dependent on the location of the tumor, due to differences in physiology, protein expression profiles, microbiome and resident immune cells along the proximal-distal axis of the colon. For example, sporadic tumors on the proximal side are more frequently diagnosed on women and people of African American descent, while at the same time they bear different molecular characteristics and exhibit a less favorable prognosis than distal colorectal tumors. Although there is extensive documentation of

genetic and environmental factors that bear an increased risk of developing CRC, the reasons by which some of them contribute to the pathology remain elusive. Positive family history accounts for approximately 10%-20% of all CRC cases and there are also known hereditary CRC syndromes accounting for about 5% of all CRC cases [46]. An increased risk of developing sporadic CRC can be observed in patients suffering from inflammatory bowel disease (IBD) [49], due to the long term colitis and associated dysbiosis and disruption of tissue homeostasis, a condition termed colitis-associated colorectal cancer (CAC). Even more, prolonged inflammation in the intestinal mucosa may be prompting to chromosomal and microsatellite instability and DNA hypermethylation, before any histologic evidence of neoplasia. Additionally, other hypotheses suggest that oxidative stress can promote macromolecular damage and disrupting the regulation of tumor suppressor proteins like p53, or proteins that participate in DNA repair mechanisms, while at the same time pro-inflammatory cytokines and altered bacterial flora of the inflamed intestine can have a significant effect in promoting anti-apoptotic signaling and exacerbating the inflammation of the intestinal epithelium, thus contributing to both colitis development and colon carcinogenesis[50].

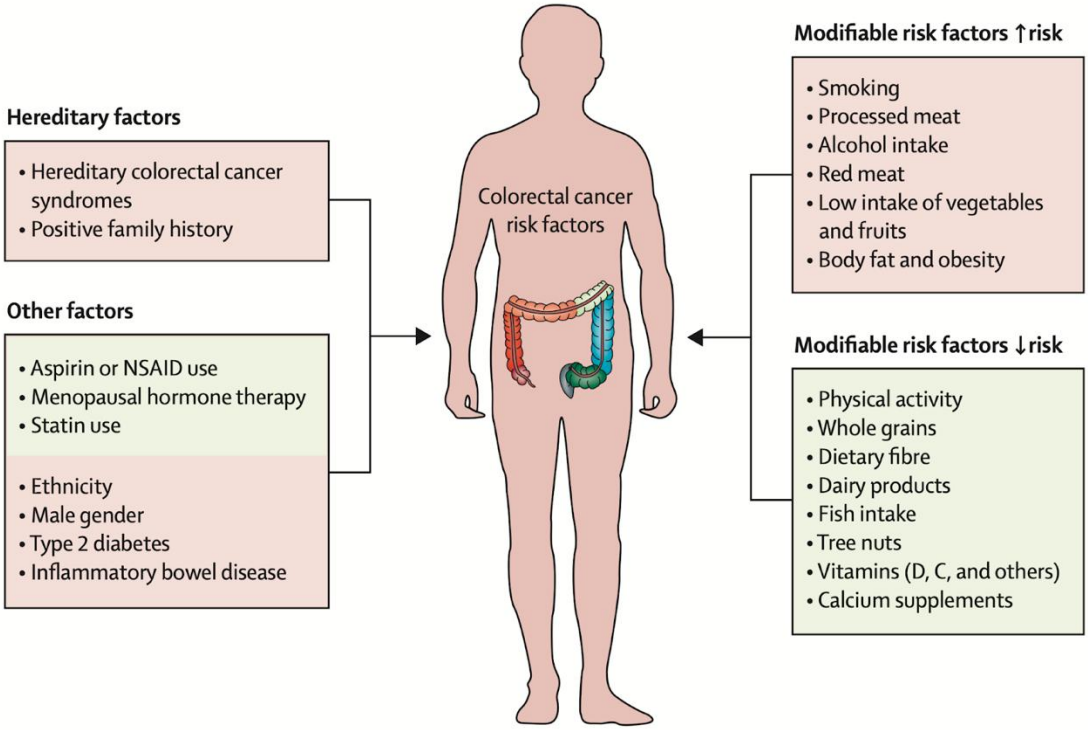

Figure 4. Risk factors for colorectal cancer. **Dekker et al. Lancet 2019.**

1.3.2 Disease progression

Colorectal cancer is a result of accumulating genetic lesions and epigenetic alterations that result in the activation and inactivation of key oncogenes and tumor-suppressor genes respectively. The most common pathway which describes the majority of CRC is known as the adenoma–carcinoma pathway, in which CRC is initiated through a neoplastic polyp, which occurs from a dysplastic crypt and will eventually form a precancerous adenoma [46]. Subsequently, cancer cells accumulate mutations over a period of 10-15 years, until the progression to an invasive carcinoma that may eventually metastasize to other parts of the organism with liver and peritoneum the most common (**Figure 5**) [47]. Even though the accumulation of genetic lesions occurs in a stochastic way as part of cancer's

evolution, there are some common recurrent genetic and epigenetic alterations, which occur in a sequential order, to drive development of CRC. In the adenoma–carcinoma model, inactivation of APC preludes the formation of an adenoma and chromosomal instability, followed by a loss of function of TP53 and activating mutation of KRAS, which is usually strong evidence for metastatic disease [46,47]. Another less frequent pathway is the serrated neoplasia pathway, which rarely exhibits APC mutations, but it is instead based on BRAS and KRAF mutations, along with increased epigenetic instability, through CpG island methylation and development of tumors either, microsatellite stable or unstable, unlike the microsatellite stable tumors developed through the adenoma–carcinoma pathway [46,47]. On the other hand, Lynch syndrome, a hereditary type of CRC, is based on germline mutations in mismatch repair (MMR) genes and results in cancers with microsatellite instability [46]. Early-stage CRC polyps can easily be dealt with through surgery, however it is very challenging cure a metastatic CRC due to its high dissemination on multiple organs [51], owing to CRC as a one of the 3 more frequent cause of cancer-related mortality. One of the main areas of investigation is to identify the subset of cells driving development of metastases. For example, a recent study showed that the majority of cancer cells that initiate metastasis are Lgr5-negative [52], an initially “paradoxical finding” since Lgr5-positive intestinal stem cells are responsible for replenishing epithelial cells colonic cells and maintain crypt architecture[53]. it is possible in cancer Lgr5-positive cancer stem cells maintain the dynamic to expand the epithelial compartment in a less controlled manner and drive tumor cells expansion [54] and even establishment of metastatic tumor in distant areas such as in the liver. In another study, disease relapse was prevented by targeting a subpopulation of CRC cells that bore mutations associated with poor prognosis, through targeting the epithelial membrane protein 1 (EMP1), showing that only the EMP1 positive cells of that subpopulation had the ability to invade and metastasize in the liver post surgery [55]. Another important factor to consider in that context is the epithelial-mesenchymal transition (EMT), a process in which cells acquire invasive capabilities by abandoning their epithelial properties in favor of a mesenchymal character [51]. Surprisingly, the majority of CRC cell lines tend to have a phenotype of partial EMT, a state in which the epithelial program is not transcriptionally repressed but rather there is an internalization of epithelial protein markers, which facilitates the migration of CRC cells in clusters instead of single cells [56]. Therefore, it is evident that delineation of the mechanistic principles behind CRC metastasis could contribute to identification of the subset of the populations with metastatic potential, required for development of targeted therapeutics with better possibilities for high efficacy and safety profiling.

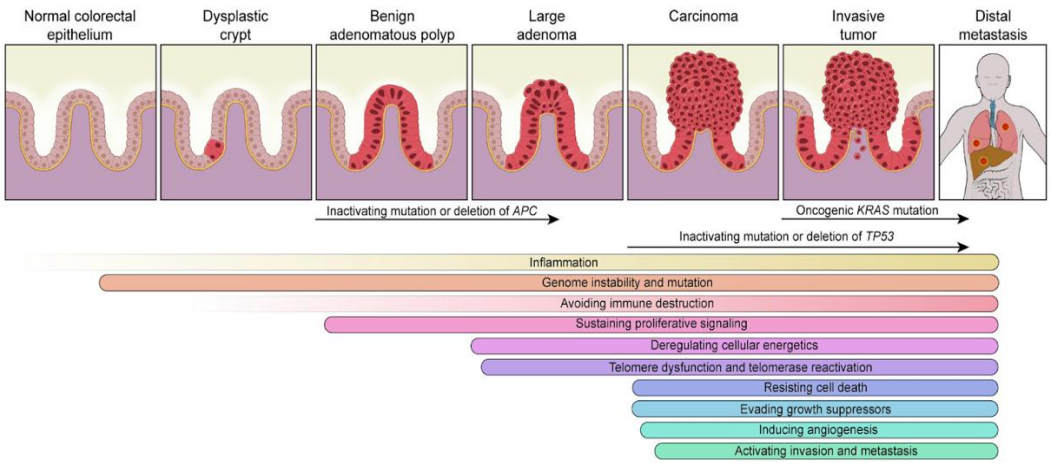

Figure 5. Progression of CRC. **Li et al. Genes & Dev. 2021.**

1.4 Modeling the intestine on a chip

1.4.1 Conventional models of the gut

The intestinal tract is a dynamic environment with a diverse microbiome and a crucial role in nutrient absorption, waste elimination, immune defense and water and electrolyte homeostasis. It is also a unique tissue with the highest self-renewal rate throughout life in mammals, thanks to the presence of the long-lived LGR5+ intestinal stem cells (ICI) residing at the bottom of the crypt. These cells are constantly dividing in a programmed manner, to generate all the cell types in the intestinal epithelium, while other quiescent stem cells in a different crypt position are responsible for the restitution of the epithelium following catastrophic injuries [57]. It seems though, that the intestinal stem cell compartment is also vulnerable to a variety of pathologies, such as cancer, infections and chronic inflammation contributing significantly in the progression and chronicity of these diseases. To shed light on the molecular mechanisms underlying gastrointestinal diseases and develop novel therapeutics, it is necessary that the physiology and function of the intestine be further elucidates. There are numerous animal models designed to study GI physiology and the pathogenesis of intestinal diseases, such as genetic intestinal epithelial disorders (congenital diarrheas and enteropathies, CODEs), Inflammatory Bowel Diseases (IBD) and CRC [34,58–60]. CRC in particular, has been studied through genetically engineered, spontaneous or inducible animal models of disease, or through the transplantation of syngeneic and patient derived cancer cells [2,60]. However, each of these “non-human” models focuses on a specific biological aspect of the disease and so far, there is no an ideal animal model to fully recapitulate critical aspects of human disease. A common way to model the intestine in vitro is via leverage of Transwell cultures, where a monolayer of intestinal cells grows on top of a permeable membrane, in order to assess the permeability of the intestinal barrier, a feature that has been used to study drug absorption [61,62]. These models usually utilize a monolayer of immortalized intestinal cell lines, with Caco-2 being one of the most prominent models of the small intestine, even though it lacks 3D cellular architecture and a relevant distribution of cell types across the intestine, while at the same time it represents a model with significantly altered expression profiles in comparison to the in vivo tissue [63]. A more recent, novel way to develop in vitro models for GI is by using intestinal organoids, which can be generated from a single crypt base columnar $LGR5^{+}$ intestinal stem cell, in the presence of the required growth factors [25]. Intestinal organoids take the form of a closed circular villus-like epithelium, resembling the intestinal crypts, but with an epithelial cells-formed enclosed lumen, and thus with reverse polarity from the cells in vivo . These organoids can be preserved in long-term cultures with an unaltered molecular profile and even though they are heterogenous and heavily dependent on the constant administration of growth factors, the fact that they display a 3D architecture mimicking the structure of the original tissue makes it a model with increased functional and physiological relevance. However, their morphology renders access to the apical side impossible, due

to their enclosed lumen, while at the same time they absorb oxygen and nutrients strictly through diffusion and they offer a model primarily for the epithelialcompartment alone [64]. The lack of access to the luminal side of the organoids can be bypassed through the use of Transwell systems, as it has been used to model intestinal infection [65], while they have also been used in the context of inflammation to study the the integrity of intestinal barrier, the disruption of which is a hallmark of IBD [66–68]. However, even the addition of organoids into Transwell platforms cannot make up for the lack of a relevant microenvironment not favored in a static culture.

1.4.2 Novel ways of culture for better in vivo/in vitro relevance

Microphysiological systems are emerging platforms aiming to overcome the caveats of static organoid and Transwell cultures, by providing a dynamic microenvironment, resembling the in vivo state. An example of microfluidic organ chips outperforming static cultures is provided by studying host-microbiota interactions, which cannot be successfully done in static cultures, mainly due to the overgrowth of bacteria and consequently the associated death of intestinal epithelial cells [64]. On the contrary, constant fluid flow on a gut-on-chip model prevented bacterial overgrowth by repelling non-attached bacteria and diluting acidic metabolites. Interestingly, in a gut-on-chip model co-culturing the probiotic *Lactobacillus rhamnosus GG* with CaCo-2 cells demonstrated increased barrier integrity, measured through transepithelial electrical resistance, thus giving insights on how biochemical cues from certain microbial strains help to improve the overall health of the intestine [64,69]. Another CaCo-2 based gut-on-chip has been developed in the context of *Shigella flexneri* infection, which is usually studied on Transwell Caco-2 cultures but with a relatively low yield [70]. This chip model provided important insights on how the infection of the apical side by microorganism in question was heavily dependent on the crypt structures of the intestinal epithelium, but also on the mechanical forces caused by intestinal peristalsis. In order to make up for the limitations of cell lines in microfluidic chips, organoids have been used to develop epithelia monolayers, by fragmenting them and seeding on a chamber coated with tissue-relevant ECM. First a Small Intestine-on-Chip was made with healthy biopsy derived organoids from duodenum, using Emulate Inc. Organ-on-Chip platform (**Figure 5**). In this system human intestinal microvascular endothelial cells (HIMECS) are seeded in opposition of the epithelium, on the “vascular side” of the porous flexible poly-dimethylsiloxane (PDMS) membrane, adding yet another in vivo relevant element into the organ model that enhanced the formation of the intestinal barrier [44]. This organoid-derived Intestine-on-Chip with continuous fluid flow and peristalsis-like mechanical forces seemed to recapitulate intestinal cellular architecture, differentiation and function, as evidenced from the 3D epithelial villi-structures, the presence of multiple intestinal epithelial cell type markers, mucus production, barrier function and digestive enzyme activity [44]. Furthermore, increased differentiation was observed as shown by the downregulation of Lgr5, indicative for stem cells, and the parallel increase in the expression of the intestinal epithelial cellular markers for Paneth cells,

absorptive enterocytes, goblet cells and enteroendocrine cells, either through the upregulation of their respective markers or via immunofluorescence microscopy. Additionally, the overall functional characteristics and transcriptomic profile of this model was significantly more relevant to an in vivo intestine than Caco-2 based organ-on-chips or plain intestinal organoids in static cultures [44]. In subsequent research, Duodenum chips were developed using 3 different adult-derived biopsies to confirm reproducibility and robustness of the system. In addition the increased relevancy of the model for drug metabolism studies was demonstrated, supporting its potential as a preclinical model to investigate pharmacokinetics and drug-drug interactions [71]. The same microfluidic system has been successfully applied to model the colon, co-culturing colon derived organoids with colon-specific HIMECs. Once again the advantage of HIMECs in improving the integrity of the intestinal barrier, as measured by dextran permeability and the formation of tight junctions, was shown via comparison of epithelial cells on chips in the presence or absence of the endothelium, including phenotypic and transcriptomic profiling [72]. This Colon-on-Chip was used as a model of barrier disruption in inflammatory settings by the prototypic cytokine, interferon-gamma (IFN-γ). The model tested in the presence of IL22 and revealed a new role for IL22 as a disruptor of the epithelial monolayer, a significant finding given the ambiguous role of IL22 in mouse colitis models, acting as a protector and deteriorator for the pathology [72]. These data highlight the importance of humanized in vitro models for the understanding of the molecular mechanisms underlying disease, as the above described intestinal inflammatory diseases. Finally, Organs-on-Chip platforms have been used in the context of CRC in an effort to reconstruct the tumor microenvironment, where enhanced tumor invasiveness was observed in the presence of both the endothelium and cancer-associated fibroblasts [73], and they have even been combined with patient-derived organoids to evaluate the effect of neurotransmitter signaling and mechanical forces on the invasiveness of the disease [74]. Modeling of cancer on chip, including CRC, is under continuous development in order to capture the complex interactions between epithelial, endothelial, stromal and immune cells and support the development of immune-oncology therapeutics taken into consideration the tumor microenvironment. In conclusion, the reconstruction of the intestinal tract on a chip heralds a unique the coming of new discoveries in the field of gastrointestinal physiology and disease, due to the to the ability of recapitulating aspects of the tissue microenvironment, that could be personalized in support of precision medicine approaches to cancer therapy.

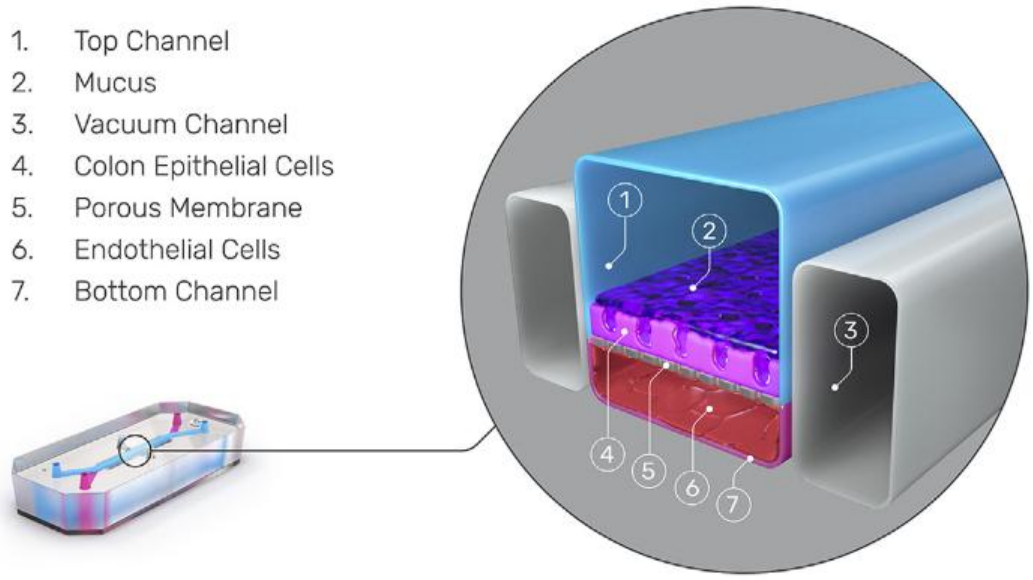

Figure 6. Schematic of the Emulate Colon Intestine-on-Chip. **Apostolou et al. Cellular and Molecular Gastroenterology and Hepatology 2021**

2. Aim of the study

The aim of the study was to develop and compare colon cancer chip models using multiple lines of patient-derived human colon organoids, and compare key phenotypic hallmarks characteristic of each condition, via immunofluorescent staining and confocal microscopy. Additionally, a colon model of PBMC recruitment was developed, with the goal of using it to study CRC treatments that rely on the presence of immune cells. Collectively, we aspire to provide an alternative in vitro model of human intestinal health and disease that will assist in the translation of scientific advancements to drug development.

3. Materials and Methods

3.1 Organoid Culture

3.1.1 CRC Organoids

Four different patient derived CRC cell lines, each with a unique mutational background (**Table 1**) were used for the culture of CRC organoids. The organoids were cultured under the manufacturer's instructions and then seeded into the top channel of the Emulate Organ-on-Chips. Specifically, each vial containing CRC organoids were thawed and then transferred in a new tube with 10mL of pre-warmed base media, which was prepared by adding 5mL of HPES, 5mL of Glutamax and 5mL of Penicillin/Streptomycin into a 500mL bottle of DMEM/F12 Plus Basal Medium. Afterwards, the tubes were centrifuged at 100g for 5 minutes and resuspended in 10mL of base media, at a density of 10000 organoids/mL. Subsequently, the desired volume was transferred to a 15mL tube pre-coated with 1%BSA and was by resuspension with 10mL media and another centrifugation at 200g for 5 minutes. The supernatant was then aspirated, leaving behind 50µL, and the organoids were resuspended with a solution of 80% Matrigel and 20% base media on ice, to prevent Matrigel from solidifying. Organoids were plated in 24-well plates, dispensing two 20µL drops of organoid Matrigel suspension per well, which would form a dome shaped matrix that would solidify after incubating the plate for 10 minutes at 37°C. To prevent edge effect, the Matrigel drops were not added to the outer wells of the plate. The cultures were fed with 1ml of complete media, made of 48.38 mL of Advanced DMEM/F12 Plus Basal Media, 0.5 mL of N2, 1 mL of B27 and 0.125 mL of N-acetyl cysteine, but with the addition of ROCK inhibitor, a factor that inhibits apoptosis and promotes cell survival, at a final concentration of 10 µM. After 2 days of culture, media was replaced every 2-3 days using complete media, without the ROCK inhibitor supplement. Additionally, PBS was added on each unused edge well. Once the organoids grew at a desired density, they were seeded on the Emulate Organ-on-Chip platforms at around 7-10 days post thaw.

Gene	Line A	Line B	Line C	Line D
APC	E1451*	G1339Ffs*2	R1450* A1446Lfs*27	Q1096 E1408
KRAS			G12D	G13D
TP53		C238Y	R248Q	R248W
BRAF	K601E			
PK3CA			E542K	
FBXW7			R465C	
SMAD4		D537H		Q534*

Table 1. Mutational background of the CRC lines.

The following reagents were used for culturing the CRC organoids:

Reagents	Vendor	Cat#
Growth factor reduced Matrigel®	Corning	356231
PBS	Sigma-Aldrich	D8537
Bovine Serum Albumin (BSA)	Sigma-Aldrich	A9418
DMEM/F-12 PLUS Basal Medium	Sigma-Aldrich	SCM162
Glutamax™ (100X)	Invitrogen	35050-079
HEPES (1M)	Sigma-Aldrich	H0887
Penicillin/Streptomycin (100X)	Sigma-Aldrich	P4333
B27 (50X)	Invitrogen	17504-044
N2 (100X)	Invitrogen	17502-048
N-Acetylcysteine (500 mM)	Sigma-Aldrich	A9165-5G
Rho Kinase Inhibitor	Sigma-Aldrich	688002

Table 2. Reagents used for the culture of CRC organoids.

3.1.2 Colon Organoids

Patient-derived colon organoids were used that were obtained from the University of Michigan. Colon organoids were thawed and plated on 24-well plates in two 20µL drops of Matrigel per well, which formed dome shaped matrices according to the provided protocols by University of Michigan. The medium used was a combination of the Intesticult medium (15%) and a complete media (85%), which is composed of 50mL of L-WRN Conditioned Medium and 50mL of 2X intestinal Media Supplement (**Table 4**). To help the recovery of the organoids post thaw, ROCK and CHIR were added to the media at the final concentration of 10µM and 3µM respectively. Colon organoids were passaged every 7-14 days whenever they reached confluency and they were passaged until they reached the demanded amount for seeding on a chip. Passaging of colon organoids was done aspirating the media and adding 500µL of cold cell recovery solution on each well. After pipetting up and down each well and making sure that the Matrigel domes were fully dissolved, all solutions were transferred to a cold low-bind protein tube for a 45-minute incubation on ice. The Matrigel/cell recovery solution would then be discarded after a centrifugation for 5 minutes at 500g and at a temperature of 4°C. Subsequently, the pellet containing the organoids would be resuspended at 3mL of media for a final wash. After another round of centrifugation with the same settings, the supernatant would be aspirated and replaced by a Matrigel solution at a final concentration of 8 mg/ml on ice to prevent it from solidifying. The Matrigel-media mix containing would then be seeded on new 24-well plates, by adding two 20 µL drops on each well, which would form dome shaped matrices that would polymerize after incubating the plates for 10 minutes at 37°C. Finally, each well containing organoids would be filled with 1mL of medium that was replaced every 2 days.

The following reagents were used for culturing the colon organoids:

Reagents	Vendor	Cat#
Growth factor reduced Matrigel®	Corning	356231
Intesticult Human Organoid Growth Medium	Stem Cell Technologies	06010
L-WRN Conditioned Medium	Sigma-Aldrich	SCM162
Cell recovery solution	Corning	354253
Rho Kinase Inhibitor	Sigma-Aldrich	688002
CHIR00-21	Reprocell	04-0004-10

Table 3. Reagents used for the culture of colon organoids.

Components	Vendor	Cat#	Volume
DMEM/F12 Plus Basal Medium	Sigma-Aldrich	SCM162	42.6 mL
N-2 Supplement (100X)	Thermo Fisher Scientific	17502048	1 mL
B-27TM Supplement (50X), without vitamin A	Thermo Fisher Scientific	12587010	2 mL
L-Glutamine Solution (100X), 200 mM	Sigma-Aldrich	TMS-002-C	1 mL
HEPES Solution, 1M in water	Sigma-Aldrich	H0887	1 mL
Niacinamide, prepared as 1M solution in water	Sigma-Aldrich	N0636	1 mL
N-Acetyl-L-cysteine, prepared as 500 mM solution in water	Sigma-Aldrich	A9165	200 mL
Human EGF, reconstituted to 200 µg/mL in PBS/ 0.1% BSA	Sigma-Aldrich	E9644	50 µL
[Leu15]-Gastrin I, reconstituted to 100 µM in PBS/ 0.1% BSA	Sigma-Aldrich	G9145	1 µL
Prostaglandin E2, reconstituted to 100 µM in DMSO	Sigma-Aldrich	P6532	1 µL
A-83-01, reconstituted to 1 mM in DMSO	Sigma-Aldrich	SML0788	50 µL
SB202190, reconstituted to 20 mM in DMSO	Sigma-Aldrich	S7067	50 µL
Penicillin-Streptomycin, 100x solution	Sigma-Aldrich	P4333	1 mL

Table 4. Components of the 2X Intestinal Media Supplement.

3.2 Establishment of Organoids-on-chip systems

3.2.1 Culture Protocol

The development of organoids-on-chip models using colon and CRC organoids (**Table 10**) was conducted according to the instructions of the Colon Intestine-Chip Culture Protocol, developed by Emulate (https://emulatebio.com/wp-content/uploads/2021/06/EP203v1.0ColonIntestine-ChipCultureProtocol.pdf) and according to previous publications[72]. The Emulate Colon Intestine-Chip is composed of two different channels separated by a porous PDMS membrane. The top channel, which hosts the epithelial intestinal cells, has a volume of 28.041 µL, an area of 20mm^2 for cells to occupy and its width and height are 1000 µm each. The bottom channel, which is where the endothelial cells reside, has dimensions of 1000 x 200 µm (width x height), a cell culture surface area of 24,4mm^2 and a total volume of 5.584 µL. Lastly, the chip contains two ports in which vacuum is applied (**Figure 7**). The establishment of the entire culture is a multistep procedure spanning multiple days, the timeline of which is briefly described below.

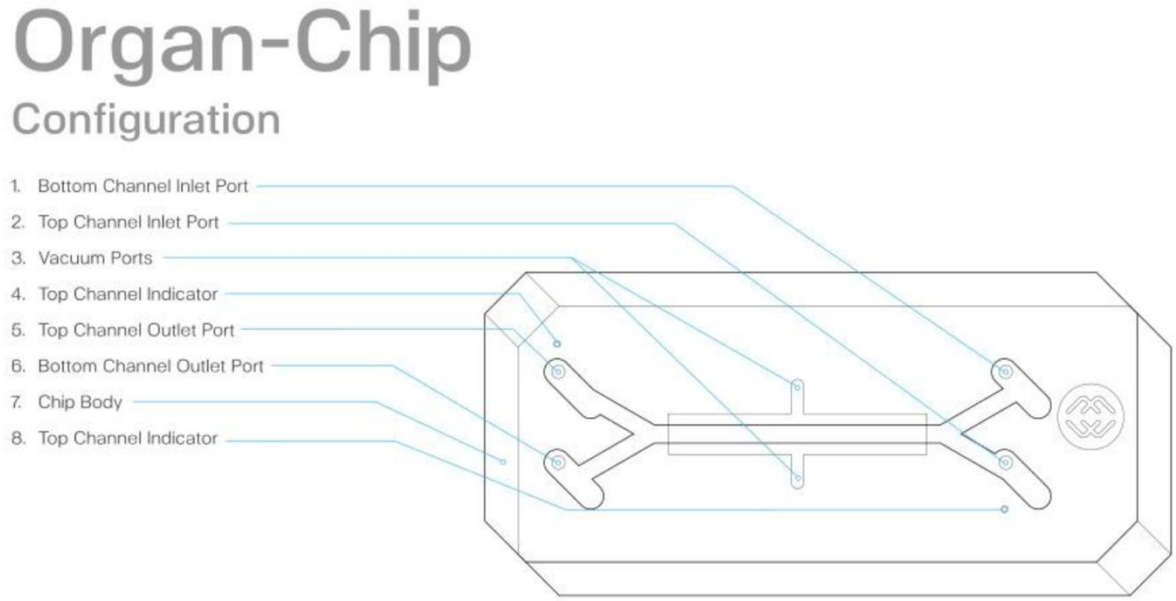

Figure 7. Configuration of the Emulate Organ-on-Chip platform (Colon Intestine-Chip Culture Protocol, EP203 v1.0, Emulate, March 19, 2021).

Day -7
Thaw human intestinal microvascular endothelial cells (HIMEC) and let them undergo expansion for at least one passage before seeding them on a chip. HIMECs will be used to form the endothelial compartment of the intestine at the bottom channel side of the chip's porous membrane, supporting the

formation of the epithelial intestinal barrier and providing in vivo relevant cell-cell interactions.

Day -1

Subsequently, the chips had to be prepared by loading them appropriately in their carriers and introducing a freshly prepared ER-1, made by combining ER-2 solution with ER-1 powder, in the bottom and top channels of each chip, without introducing bubbles to the channels, followed by the activation of ER-1 coated chips under UV light for 15 minutes. The use of freshly made ER-1 solutions is of utmost importance and the chip culture would fail otherwise. Subsequently, the ER-1 solution is fully aspirated, and the chip channels are washed with ER-2 and then DPBS, before being coated with an ECM made of Collagen IV and Matrigel or Fibronectin for the top or bottom channel respectively.

Day 0

The next day, HIMEC cells were suspended in Complete HIMEC Culture Medium at a concentration of 8-10 million cells per mL and then seeded on the bottom channel of each chip. After confirming the correct cell density on the microscope and approximately 1-hour post-seeding, the bottom channels were washed with Complete HIMEC Culture Medium, while the top channels were washed using their corresponding organoid culture media to prevent them from drying out. Subsequently, the organoids were seeded on the top channel of each chip, after being recovered from Matrigel using a Cell Recovery solution and fragmented via the use of a TrypLE digestion solution, diluted with DPBS on a 1:1 ratio and supplemented by 2μL of ROCK inhibitor (Y-27632). The fragmented organoids were transferred to the chips at a seeding density of approximately 7 million cells per mL, in a solution of the medium used throughout their culture, supplemented by Y-27632 and CHIR99021 to increase their viability. Media would be replenished on a regular basis for both channels but the addition of Y-27632 and CHIR99021 on the top channel would cease after day 1 post-seeding.

Day 1

The next day after seeding, each channel was washed with its corresponding medium to eliminate all nonadherent cells. All media that was used on this step, but also for the rest of the protocol, underwent gas equilibration via Steriflip Vacuum Tube Filters (provided by Millipore, Cat# SE1M003M00), to prevent the formation of bubbles in the chip or any of the instruments used, which would negatively impact the viability of cells and the regular fluid flow. Dextran, a fluorescent tracer, was also included in the equilibrated organoid media to assess the permeability of the intestinal barrier throughout the culture. Afterwards, the chips were loaded into Pods that would allow the connection of the chip cultures to the Zoë Culture Module, an automated system that recreates the in vivo microenvironment by providing a continuous dynamic flow of media and the mechanical forces. This system can simultaneously sustain up to 12 different chips and it is connected to an Orb Hub module, which is responsible for providing power, vacuum stretch and gas supply of 5% CO_2. The system was set to provide a medium flow rate of 30 μL per hour for both channels.

Day 2
Each medium was replenished on the next day for both channels but without the addition of Y-27632 and CHIR99021. Additionally, 50μL of Effluents were also collected for the media in the inlet and outlet of each channel in the Pod's reservoirs, to assess the permeability of Dextran and thus formation of the intestinal barrier, via a Spectrophotometer Microplate Reader. Effluent sampling would thereafter be conducted on each day of the culture.

Day 3
The system was set to provide the chips with a 2% stretch at a frequency of 0.15 Hz.

Day 4
Stretching was increased to 10% at a frequency of 0.15 Hz.

Day 5-9
Effluent sampling was performed daily and culture media was refreshed every other day, until ready to be stained.

Reagents	**Vendor**	**Cat#**
Growth factor reduced Matrigel®	Corning	356231
Collagen IV	Sigma-Aldrich	C5533
Fibronectin	Corning	356008
Y-27632 (ROCK inhibitor)	Stem Cell Technologies	72304
CHIR00-21	Reprocell	04-0004-10
Cell Recovery Solution	Corning	354253
ER-1	Emulate	-
ER-2	Emulate	-
Dulbecco's PBS (DPBS), without Ca^{+2} and Mg^{+2}	Corning	21-031-CV
Trypan blue	Sigma-Aldrich	93595
TrypLE Express	Thermo Fisher Scientific	12604013
Advanced DMEM/F12	Thermo Fisher Scientific	12634028
Intesticult™ Human Organoid Growth Medium	Stem Cell Technologies	06010
2X intestinal Media Supplement	-	-
L-WRN Conditioned Medium	Sigma-Aldrich	SCM162
Endothelial Cell Growth Medium MV 2	Promocell	C-22121
Fetal bovine serum (FBS)	Sigma-Aldrich	F4135
Primocin	InvivoGen	ANT-PM-1
Attachment Factor™	Cell Systems	4Z0-210

Reagents	Vendor	Cat#
BSA	Sigma-Aldrich	D2650
3KDa Dextran Cascade Blue	Invitrogen	D7132
Cascade Blue	Invitrogen	C687
Lucifer Yellow	Invitrogen	D3329

Table 5. Reagents used for the culture and the development of the organoids-on-chips, based on the Colon Intestine-Chip Culture Protocol by Emulate.

3.2.2 Proinflammatory Cytokines and Seeding of PBMCs

Proinflammatory Cytokines, chemokines and PBMCs were seeded on organoids-on-chips according to Emulate's protocol, titled "Basolateral Recruitment of Peripheral Blood Mononuclear Cells (PBMCs) on the Colon Intestine-Chip"(https://emulatebio.wpenginepowered.com/wp-content/uploads/2022/06/Emulate-EP215-Rev-A_Basolateral-Recruitment-of-PBMCs-on-the-Colon-Intestine-Chip.pdf). TNF-α and gut-specific chemokines were introduced to regular colon chips, in order to create the inflammatory conditions necessary for the recruitment of PBMCs to the site of inflammation and induce the disruption of the barrier. Specifically, priming of the chips was conducted on day 5, after a mature enough barrier had been formed (Papp ≤ 1x10-6 cm/s). Cells of the endothelial channel were treated with TNF-α for 24h, while the epithelial channel was treated with chemoattractant chemokines. Both the treatments were prepared according to Emulate's protocol in the medium given to their respective channels at a concentration of 50ng/mL.

Reagents	Vendor	Cat#
Cell culture grade water	-	-
BSA	Sigma-Aldrich	A7030
Dulbecco's Phosphate Buffered Saline 1X	Sigma-Aldrich	D8537
Primocin	VWR	MSPP-ANTPM-1
TNF-α	R&D Systems	210-TA-020
Recombinant human IP-10 (CXCL10)	PeproTech	300-12
Recombinant human MIP-3a (CCL20)	PeproTech	300-29A
Recombinant human MEC (CCL28)	PeproTech	300-57
Recombinant human GPR15L	PeproTech	300-71
Recombinant human TECK (CCL25)	PeproTech	300-45
Recombinant human MCP-1 (CCL2)	PeproTech	300-04
Recombinant human SDF-1α (CXCL12)	PeproTech	300-28A
Recombinant human MIP-3β (CCL19)	PeproTech	300-29B
Recombinant human IFN-γ	PeproTech	300-02

Table 6. Materials required for the treatment of TNF-α, IFN-γ and Chemoattractant cocktail.

IFN-γ was administered on the endothelial channel of the CRC chips with a goal to stimulate the disruption of the intestinal barrier. The treatment took

place on day 5 of culture, after the formation of a mature barrier for 24h. IFN-γ was administered through the culture medium of the bottom channel in the concentration of 100ng/mL and the medium was replenished every 24h.

3.2.3 Culture and recruitment of PBMCs

PBMCs were introduced to the chips 24 hours after priming (day 6) for 4 hours before washing and replenishing the culture medium, following the manufacturer's instructions (https://emulatebio.wpenginepowered.com/wp-content/uploads/2022/06/Emulate-EP215-Rev-A_Basolateral-Recruitment-of-PBMCs-on-the-Colon-Intestine-Chip.pdf).

Reagents	Vendor	Cat#
Cell culture grade water	-	-
α4 integrin small molecule inhibitor (AJM300, carotegrast methyl; MedChemExpress, Cat. HY-124290)	MedChemExpress	HY-124290
Human Peripheral Blood Mononuclear Cells, Frozen (PBMCs) (StemCell, Cat. 70025)	StemCell	70025
Cell Tracker stain (Deep Red, Thermo Fisher Scientific, Cat. C34565)	Thermo Fisher Scientific	C34565
DMSO	Sigma-Aldrich	D4540
RPMI 1640 Medium, powder, HEPES	Thermo Fisher Scientific	23400021
Sodium Bicarbonate	Sigma-Aldrich	S5761
Fetal bovine serum	Sigma-Aldrich	F4135
Pen-Strep	Sigma-Aldrich	P4333
Percoll®	Sigma-Aldrich	P4937
Gelzan™ CM	Sigma-Aldrich	G1910
Trypan Blue	Thermo Fisher Scientific	15250061

Table 7. Required Reagents for PBMC administration.

3.2.4 Barrier function analysis

The analysis of the epithelial barrier function was conducted by detecting the permeability of Dextran Cascade Blue from the dosing channel (top) to the receiving channel (bottom), through a plate reader, according to the manufacturer's instructions (https://emulatebio.wpenginepowered.com/wp-content/uploads/2021/06/EP187_v1.0_Barrier_Function_Analysis_Protocol.pd

f). For this assay, Dextran Cascade Blue treatment was administered at a size 3 kDa and a final concentration of 50 μg / mL and the permeability was calculated through the following equation:

$$P_{app} = -\frac{Q_R * Q_D}{SA * (Q_R + Q_D)} * \ln\left[1 - \frac{C_{R,0} * (Q_R + Q_D)}{(Q_R * C_{R,0} + Q_D * C_{D,0})}\right]$$

Papp is the apparent permeability (cm/s), SA is defined as the surface area of the co-culture channel (0.17cm^2), Q_R and Q_D represent the fluid flow rates in the receiving and dosing channels respectively (cm^3/s), while $C_{R,0}$ and $C_{D,0}$ are the recovered concentrations in the receiving and dosing channels respectively. This assay was conducted daily on every established chip in order to confirm and monitor the maturation of the intestinal barrier.

3.3 Immunofluorescence staining

3.3.1 Immunostaining of Colon Organoids-on-Chip

The established of the normal colon organoids chips were stained for ZO-1, Hoechst, MUCIN2, SLC26A3 to detect markers of epithelial intestinal cells. The endothelial channels of separate chips were stained for Hoechst, CD31 and VE-Cadherin to identify markers of the intestinal microvascular endothelial cells. In another experiment where an immune cell recruitment colon model was designed, the chips were stained via immunofluorescence for ZO-1, CD45 and Hoechst. Anti-CD45 antibodies were used to target peripheral blood mononuclear cells (PBMC). PBMCs were administered either on the top channel, bottom channel or none and the goal is to evaluate their effect on tight-junctions integrity, under a context of inflammation, but also to check their effect when migrating from the endothelial compartment (bottom channel) to the lumen of the intestine (top channel), further mimicking the in vivo setting. Fluorescent-dye conjugated anti-ZO-1 antibodies were used to evaluate the integrity of tight junctions in the presence of PBMCs. Finally, Hoechst was used to visualize the nuclei of cells and the cells were visualized using a Zeiss LSM 880 Confocal Microscope.

The chips were stained following the protocol as described below:

1. **Fixation**
   i. Gentle wash on both channels with 200μL Dulbecco's Phosphate Buffered Saline (DPBS).
   ii. Flush 200μL 4% Paraformaldehyde (PFA) through each channel.
   iii. Fix for 15 min at room temperature.
   iv. Flus 200μL DPBS through each channel 3 times.
   v. Place chips in DPBS until ready to stain.
2. **Blocking**
   i. Flush 200μL filtered DPBS through the staining channels.
   ii. Add 200μL pipette tips to the unstained channels.

iii. Flush through 200µL 0.1% triton + 10% Normal Goat Serum (NGS) in DPBS for 30 minutes at room temperature to permeabilize cell membranes.

iv. Wash channel 3x with DPBS.

v. Block staining channels with 200µL popette tips containing a 10% NGS in DPBS solution (gravity wash) for 2 hours at room temperature.

3. Administration of conjugated antibodies

i. Dilute the conjugated antibodies for CD45 and ZO-1 in a 5% NGS/DPBS solution master mix.

ii. Remove pipette tips from the channel.

iii. Flush through 100µL of antibody/blocking buffer.

iv. Add 200µL pipette tip and an additional 200 µL of antibody buffer to channel (gravity wash).

v. Incubation overnight on a rocker at 4°C.

vi. Flush 200 µL DPBS through the staining channels on each chip.

vii. Flush another 200µL of DPBS + 0.1% saponin (wash buffer) through the staining channel and place on rocker for 5 minutes.

viii. Repeat 2 more times, for a total of 6 washes.

4. **Secondary Antibody**

i. Dilute the secondary antibody for CD45 in a 5% NGS/DPBS solution.

ii. Flush 100µL of secondary solution through the channel.

iii. Add 200µL pipette tip and an additional 200µL secondary solution (gravity wash).

iv. Incubate at room temperature, on a rocker, in the dark for 2 hours.

v. Flush 200µL DPBS through the staining channels of the chip.

vi. Flush another 200µL wash buffer through the staining channel and place on rocker for 5 minutes. Repeat 2 more times.

vii. Add 2 drops of Hoechst solution to 1ml DPBS.

viii. Flush 200µL of Hoechst solution through the staining channels for 3 minutes. Solution is made by adding 2 drops of Hoechst to 1mL of DPBS)

ix. Flush 200µL DPBS through the staining channel.

x. Flush an additional 200µL DPBS through the staining channels and place on rocker for 5 minutes. Repeat this step 2 more times.

xi. Add 200µL of Ibidi mounting medium both channels to hold specimens in place and prevent photobleaching.

xii. Store at 4°C.

3.3.2 Immunostaining of CRC Organoids-on-Chip

The chips were stained via immunofluorescence for ZO-1, E-Cadherin and Hoechst. Anti-ZO-1 antibodies were used to evaluate the integrity of tight junctions, while anti-E-Cadherin antibodies, which also stains the tight junctions, were used to assess the EMT progression and metastatic potential of CRC cells. Finally, Hoechst was used to visualize the nuclei of cells.

The following protocol was followed:

1. Fixation

i. Gentle wash on both channels with 200µL Dulbecco's Phosphate Buffered Saline (DPBS).
ii. Flush 200µL 4% Paraformaldehyde (PFA) through each channel.
iii. Fix for 15 min at room temperature.
iv. Flus 200µL DPBS through each channel 3 times.
v. Place chips in DPBS until ready to stain.

2. Blocking

i. Flush 200µL filtered DPBS through channel.
ii. Add 200µL pipette tips to unstained channel.
iii. Flush through 200µL 0.1% triton + 10% Normal Goat Serum (NGS) in DPBS for 30 minutes at room temperature to permeabilize cell membranes.
iv. Wash channel 3x with DPBS.
v. Block top channel with 200µL popette tips containing a 10% NGS in DPBS solution (gravity wash) for 2 hours at room temperature.

3. Primary Antibody

i. Dilute the primary anti-E-Cadherin antibody and the fluorophore conjugated ZO-1 antibody in a 5% NGS/DPBS solution**.**
ii. Remove pipette tips from top channel.
iii. Flush through 100µL of antibody/blocking buffer.
iv. Add 200µL pipette tip and an additional 200 µL of antibody buffer to channel (gravity wash).
v. Incubation overnight on a rocker at 4°C.
vi. Flush 200 µL DPBS through staining channel in each chip.
vii. Flush another 200µL of DPBS + 0.1% saponin (wash buffer) through the staining channel and place on rocker for 5 minutes.
viii. Repeat 2 more times, for a total of 6 washes.

4. **Secondary Antibody**

i. Make a secondary antibody mix in a 5% NGS/DPBS solution.
ii. Flush 100µL of secondary solution through channel.
iii. Add 200µL pipette tip and an additional 200µL secondary solution (gravity wash).
iv. Incubate at room temperature, on a rocker, in the dark for 2 hours.
v. Flush 200µL DPBS through the staining channel (top channel) of the chip.
vi. Flush another 200µL wash buffer through the staining channel and place on rocker for 5 minutes. Repeat 2 more times.
vii. Add 2 drops of Hoechst solution to 1ml DPBS.
viii. Flush 200µL of Hoechst solution through the staining channel for 3 minutes. Solution is made by adding 2 drops of Hoechst to 1mL of DPBS)
ix. Flush 200µL DPBS through the staining channel.
x. Flush an additional 200µL DPBS through the staining channel and place on rocker for 5 minutes. Repeat this step 2 more times.
xi. Add 200µL of Ibidi mounting medium both channels to hold specimen in place and prevent photobleaching.
xii. Store at 4°C.

3.3.3 Immunofluorescence Reagents

The reagents listed on **Table 8.** and **Table 9.** were used for the immunofluorescent staining of the chips.

Reagents	Vendor	Cat#
1x DPBS	Corning	21-031-CV
10x DPBS	Gibco	14190-144
32% PFA	Electron Microscopy Sciences	15714
Triton-X 100	Sigma-Aldrich	-
Normal Goat Serum	Gibco	PCN5000
Hoechst	Invitrogen	R37605
Mounting medium	Ibidi	50001
Saponin	Sigma-Aldrich	SAE0073

Table 8. List of reagents for immunofluorescence.

Antibodies	Vendor	Cat#	Dilution
Anti-ZO-1 Monoclonal Antibody (ZO1-1A12), Alexa Fluor™ 594	Thermo Fisher Scientific	339194	1:100
Anti-E-Cadherin Antibody	Abcam	ab40772	1:100
NucBlue™ Live ReadyProbes™ Reagent (Hoechst 33342)	Invitrogen	R37605	-
Monoclonal rat anti-CD45	Invitrogen	MA5-17687	1:500
Mucin 2 Antibody (Ccp58) Alexa Fluor™ 594 conjugated	Santa Cruz	Sc-7314	1:100
Anti-VE-Cadherin antibody	Abcam	Ab33168	1:100
Anti-alpha 1 Sodium Potassium ATPase antibody	Abcam	Ab7671	1:100
Anti-CD31 antibody	Abcam	Ab28364	1:100
Anti-SLC26A3 antibody	Abcam	Ab244452	1:100
Alexa Fluor™ 488 Goat anti-Rabbit IgG (H+L) Secondary Antibody	Invitrogen	A11034	1:100
Alexa Fluor™ 488 Goat anti-Rat IgG (H+L) Secondary Antibody	Thermo Fisher Scientific	A-11006	1:100
Alexa Fluor™ 594 Goat anti-Mouse IgG (H+L) Secondary Antibody	Thermo Fisher Scientific	A-11005	1:100

Table 9. List of Antibodies used for immunofluorescence.

Experiment	Line	Treatment	Number of samples

IFN-γ driven epithelial barrier disruption	Colon	Control	2
		IFN-γ	2
Test for the presence of endothelial cells	Colon	Control (Check for HIMECs)	1
Test for the differentiation of colon organoids to goblet cells	Colon	Control (Test for MUC2)	1
Recruitment of PBMCs and their effect on Barrier disruption	Colon	Control	3
	Colon	TNF-α + Chemokines	2
	Colon	PBMCs (Top)	2
	Colon	PBMCs (top) TNF-α + Chemokines	2
	Colon	PBMCs (bottom) TNF-α + Chemokines	3
CRC Organoids-on-Chip	CRC Line A	Control	2
	CRC Line A	IFN-γ	1
	CRC Line C	Control	2
	CRC Line C	IFN-γ	1

Table 10. Characteristics of each stained organoids-on-chip.

3.4 Quantification of proinflammatory cytokines on chip effluents

After the initiation of stretch in the chips modeling IBD, effluents were collected daily to assess the secretion of proinflammatory cytokines. Specifically, the secretion levels of IFN-γ and IL-22 were evaluated through Enzyme-Linked Immunosorbent Assays (ELISA) following Abcam's IFN gamma Human *in vitro* ELISA kit (ab46025) and Human IL-22 SimpleStep ELISA® Kit (ab216170) protocols respectively.

4. Results

4.1 Establishment and characterization of Colon-on-chip

Colon-on-chips were established as mentioned in Material and methods (**Figure 8**). HIMEC cells were seeded in the bottom and colon organoids that were grown in 24 well plates to confluency (**Figure 9**) and were then seeded on Emulate chips as mentioned in Materials and Methods. Barrier integrity was determined from Day 2 onwards via addition of 3kDa Dextran in the medium of the top channel. Once the barrier was formed, IFN-γ (100 ng/mL), was added to the bottom channel for 72 hours. IFN-γ has been shown to compromise the intestinal epithelial barrier through by disrupting the tight-junctions and it has been associated with the pathogenesis of IBD and other inflammatory diseases [72]. As expected, we saw disruption of epithelial barrier in the presence of IFN-γ, mimicking the loss of barrier integrity in IBD.

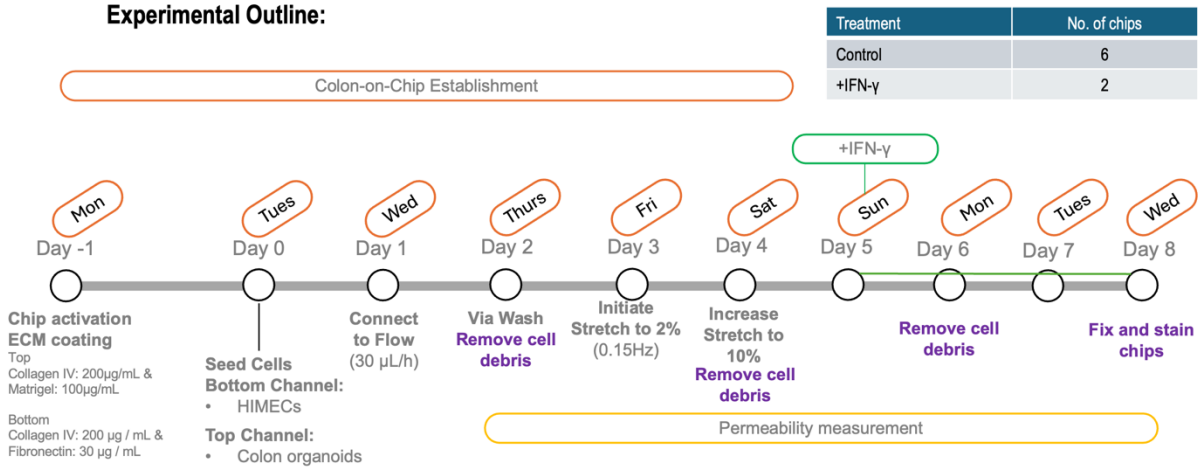

Figure 8. Experimental outline of the Colon-on-Chip establishment.

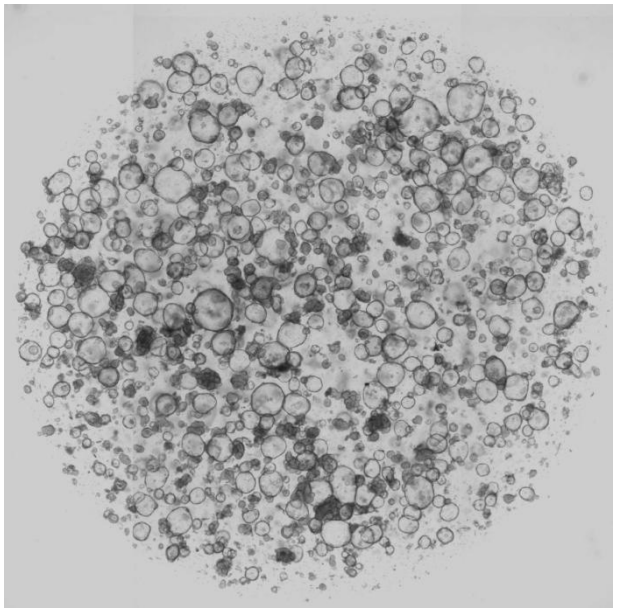

Figure 9 Representative image of a well of colon organoids embedded in matrigel (4x).

(A) Disruption of the epithelial barrier

Chips seeded with colon organoids showed significant disruption of the epithelial barrier after administering a 72-hours treatment of IFN-γ. The increased barrier permeability was confirmed both by the apparent gaps through the tissue in IFN-γ treated chips in comparison to their controls, but also by the 3 kDa Dextran permeability assay (**Figure 10.**).

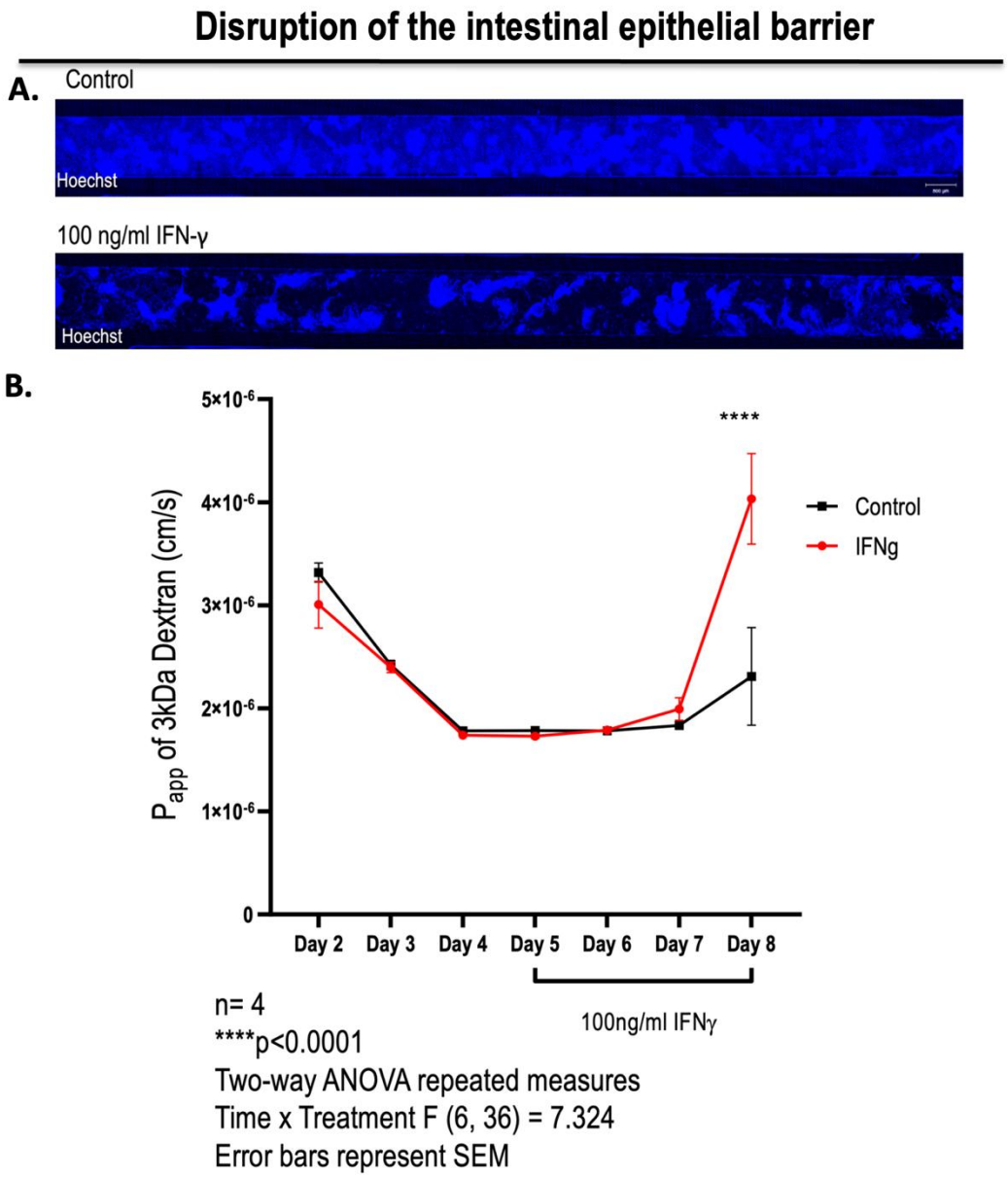

Figure 10. Disruption of the epithelial barrier in the context of IFN-γ inflammation. (A) Disorganization of the epithelial tissue in the top channel of the chip. (B) Analysis of intestinal permeability after 72 hours of 100 ng/ml IFN-γ. treatment.

(B) Confirming the presence of the endothelial compartment

VE-Cadherin is a vascular endothelial protein that plays a significant role in cell-cell adhesion used as an endothelial marker. Staining on the endothelial (bottom) channel of the chip confirmed that HIMECs (**Figure 11B**) had indeed been seeded and formed the endothelial side of the barrier, by identifying the expression of endothelial tight-junctions marker, VE-Cadherin (**Figure 11A, 11C**). Staining on another chip confirmed that HIMECs also expressed CD-31, a molecule expressed in endothelial cells and implicated in cell adhesion, signaling, angiogenesis and leukocyte transmigration.

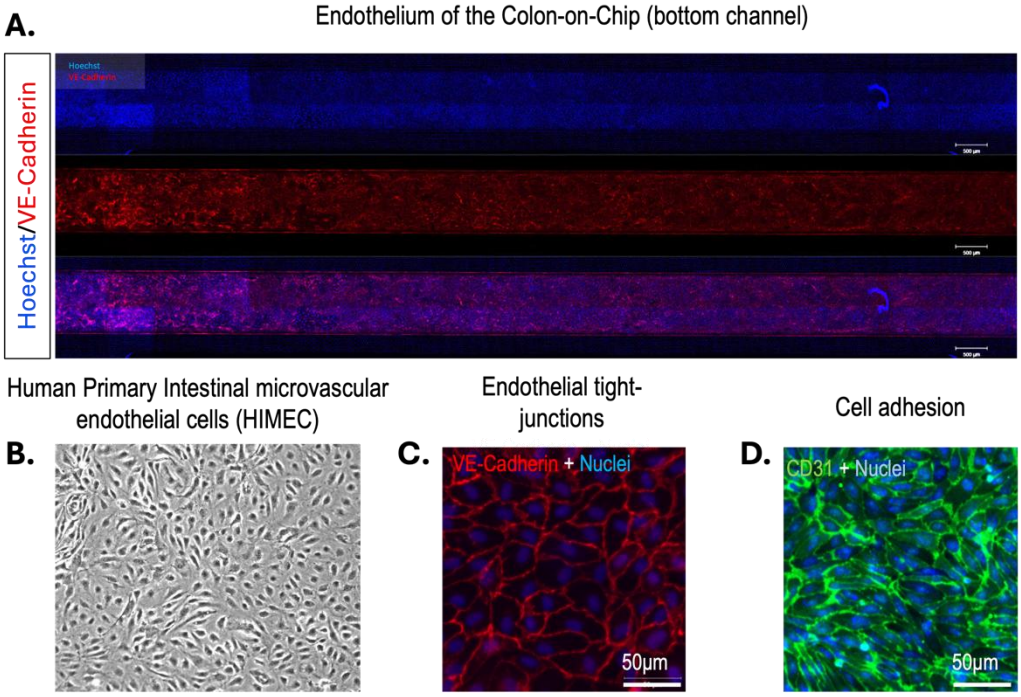

Figure 11. (A) Colonic human intestinal microvascular endothelial cells form a homogenous barrier and express VE-Cadherin throughout the endothelial channel. (Top) Hoechst (Blue), (Middle) VE-Cadherin (Red) and (Bottom) composite image. (B) Representative bright field image of the colonic cells HIMECs. (C) Representative higher magnification image of the staining (20X).

(C) Confirming the differentiation of epithelial cells

The epithelial channels of chips were stained with different markers to identify differentiated epithelial cells. Staining of MUC2 (green) aimed to identify the presence of goblet cells. We observed scattered expression of Muc2+ cells in the chip (**Figure 12B**) as shown previously [72]. MUC2 is a glycoprotein produced by goblet cells, which is a major component of the mucus layer in the intestinal tract. SLC26A3 and NA^{+}/K^{+}-ATPase, were also stained on a different chip, confirming the presence of enterocytes (**Figure 12A**). Expression of these markers in in the epithelium confirms the ability of organoids to differentiate in different epithelial cell subtypes while on the chip. Hence, the formed tissue should be capable of capturing functional indices of the in vivo intestine, through the presence of the entire repertoire of intestinal cell types, whereas each one of them has a unique function.

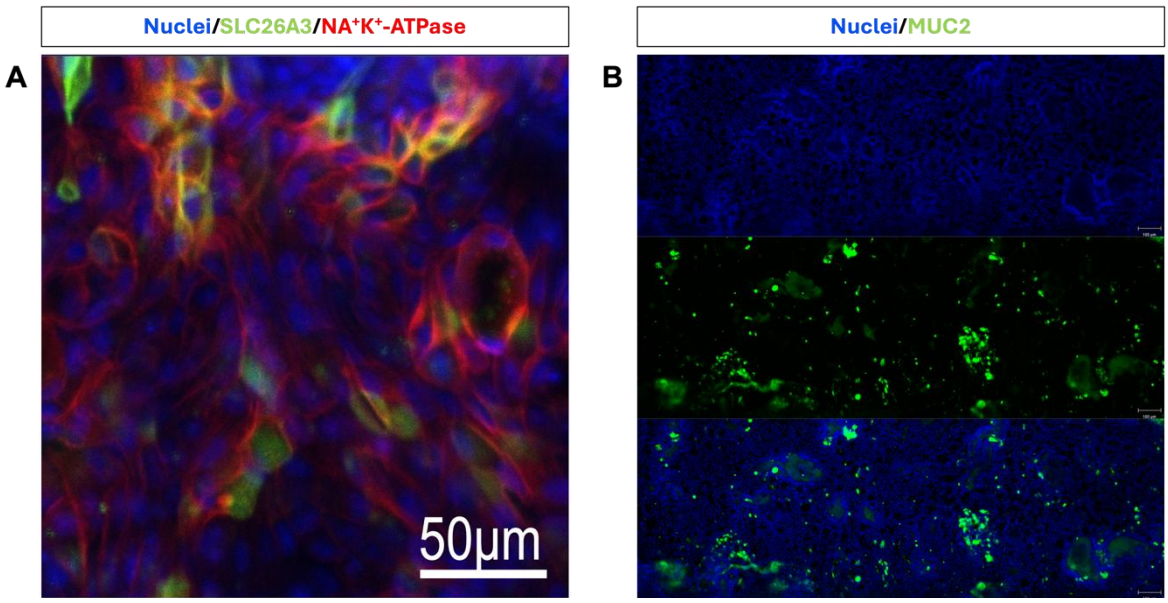

Figure 12. Differentiation of intestinal epithelial cells (A) Confirmation of differentiated enterocytes present on the chip, through the expression of SLC26A3 and NA^+/K^+-ATPase. (B) Confirmation of differentiated goblet cells present on the chip, via the expression of MUC2. Top: Hoechst staining, Middle: MUC2 staining, Bottom: composite picture.

4.2 Modeling of immune cell recruitment in the context of TNF-α induced inflammation.

The recruitment of immune cells in the intestinal tract is fundamental process for the maintenance of organismal health. These cells play a critical role in CRC, infectious diseases, IBD and other inflammatory diseases, by maintaining an environment of persisting inflammation. Understanding the mechanisms underlying immune cell recruitment and its impact on intestinal health and disease is essential for developing targeted therapies and improving clinical outcomes for patients suffering from these debilitating conditions. Thus, we developed a model of PBMC recruitment, similarly to the way it occurs in vivo, with the goal of using it to study treatments for CRC that rely on the presence of immune cells. The inflammatory conditions necessary for the recruitment of immune cells were recreated via the administration of a chemokine cocktail and TNF-α, a proinflammatory cytokine known to disrupt the tight-junctions protein ZO-1 [75,76]. The colon-on-chip was established as previously mentioned and when the barrier integrity reached the desired apparent permeability (Papp ≤ 1x10-6 cm/s), the chips were treated with either a combination of chemokines and TNF-α or TNF-α alone, as described earlier (**Figure 13D**). The next day, PBMCs were thawed and rested for 4 hours and later stained with cell tracker. They were then flowed through the chip at a flow rate of 1000ul/hour for 4 hours as shown in the outline below. (**Figure 13A**). After one day, using confocal microscopy, we observed PBMCs recruited on the top channel as expected (**Fig 13C**). 96 hours after PBMCs were flowed through, the chips were then fixed and stained for CD-45, ZO-1 and cell nuclei. Daily effluents were collected from the top and bottom outlet

and measured for release of Interferon-gamma (IFN-γ) and Interleukin-22 (IL-22).

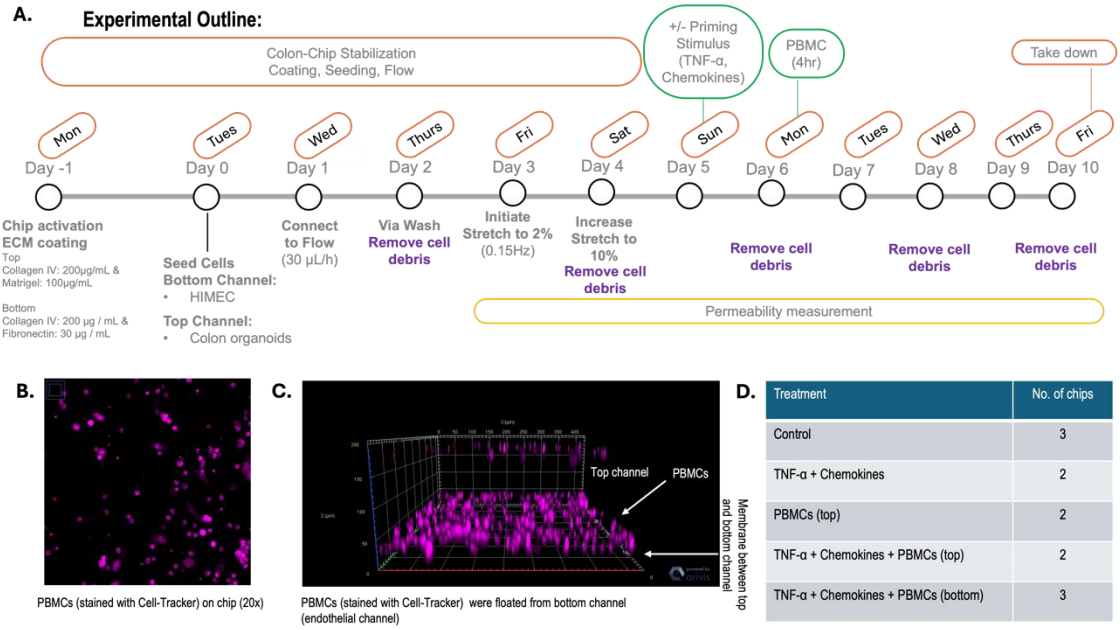

Treatment	No. of chips
Control	3
TNF-α + Chemokines	2
PBMCs (top)	2
TNF-α + Chemokines + PBMCs (top)	2
TNF-α + Chemokines + PBMCs (bottom)	3

Figure 13. Establishment of inflammation-induced PBMC recruitment on chip. (A) Experimental outline of the model. (B) Confocal microscopy picture of PBMCs on chip stained with Cell-Tracker. (C) Migration of PBMCs from the bottom to the Top Channel. (D) Treatment table of the experiment.

Using a Zeiss LSM 880 Confocal Microscope, the formation of tight junctions was evaluated, via ZO-1 staining, a feature of the intestinal epithelium that contributes to the formation of a tight and impermeable barrier. The ability of the intestinal epithelial tissue to form tight junctions during the inflammatory driven invasion of PBMCs was evaluated on six different chip cultures. The presence of inflammatory conditions led to a severe disorganization of the epithelial tight-junctions, an expected outcome considering the disruption of the intestinal barrier during chronic inflammation, a hallmark of IBD.

1. Control conditions of the experiment

On the control chips, colon organoids were cultured in the absence of a proinflammatory challenge. Well-formed tight junctions were detected (Red) as well as the nuclei of the Colon cells (blue) (**Figure 14A**). Several green spots are also observed, due to the anti-CD45 antibody, which was used on the chip, however they do not specifically bind to anything due to the absence of PBMCs in the model.

2. The effect of inflammatory environment to the intestinal epithelial barrier.

The second set of chips differs greatly from the first one, due to the administration of chemokines TNF-α through the top and bottom channels respectively (priming). This inflammatory setting seems to be responsible for

the extensive disorganization of the tight-junctions network, without the presence of PBMCs (**Fig 14B**).

3. The effect of PBMCs without priming the chips.

PBMCs, CD45-positive cells (green), were seeded on the top channel of unprimed chips, not treated with proinflammatory agents. There is clearly a higher presence of green staining, in comparison to the chips that did not have PBMCs, however the presence of these cells by themselves doesn't seem to have any significant effect on the integrity of the tight junctions and thus the intestinal epithelial barrier (**Fig 14C**).

4. Administration of PBMCs on the top channel of primed chips.

Chip with PBMCs on the top channel of the chip, in the context of TNF-α driven inflammation displayed advanced disorganization of the tight-junctions, and especially in the areas where PBMCs reside (green), while the pattern of the ZO-1 staining (red) tends to be intact in areas where PBMCs are not present (**Figure 14D**). However, the disruption of the tight-junctions network appears to be less severe than in the priming conditions without the PBMCs.

5. Administration of PBMCs on the bottom channel of primed chips.

PBMCs were introduced through the bottom channel of the chip. This key difference was made to mimic the in vivo procedure of how PBMCs migrate to the intestinal epithelium during inflammation. The PBMCs were able to invade to the top channel of the chip through the porous membrane and induce similar effect as with the previous conditions. (**Figure 14E**).

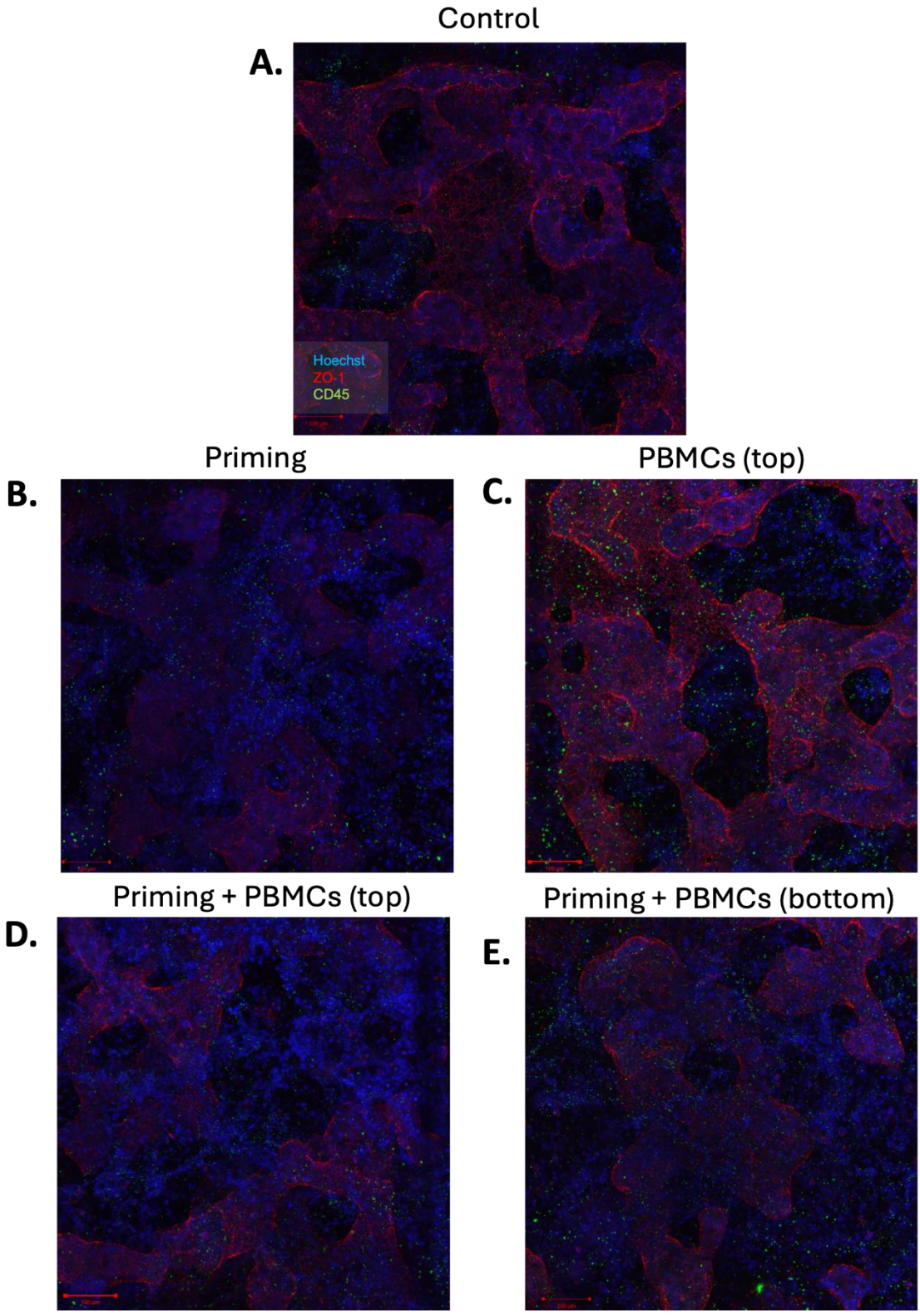

Figure 14. The effect PBMCs and TNF-driven inflammation on epithelial barrier disruption. (A) Control conditions no PBMCs and priming (with TNF-α and chemokine cocktail), in which the intestinal epithelial barrier remains unaffected, based on the staining of ZO-1. (B) Priming of chips resulted in severe disruption of the ZO-1 network. (C) No significant effect was observed on the tight-junctions network when PBMCs alone were present in the top

channel. (D) The epithelial barrier was once again disrupted, but interestingly not in the same intensity as in priming with the absence of PBMCs, however ZO-1 tends to be absent in locations where PBMCs are present. (E) When PBMCs were administrated through the bottom channel, the intestinal barrier was once again disrupted. Hoechst (Blue), ZO-1 (Red), CD45-positive PBMCs (Green).

4.2.1 Increased permeability of the intestinal barrier

The analysis of effluents from chips seeded with colon organoids, using the 3 kDa Dextran permeability assay, showed a significant disruption of the epithelial barrier after administration of TNF-α and PBMCs. (**Figure 15**).

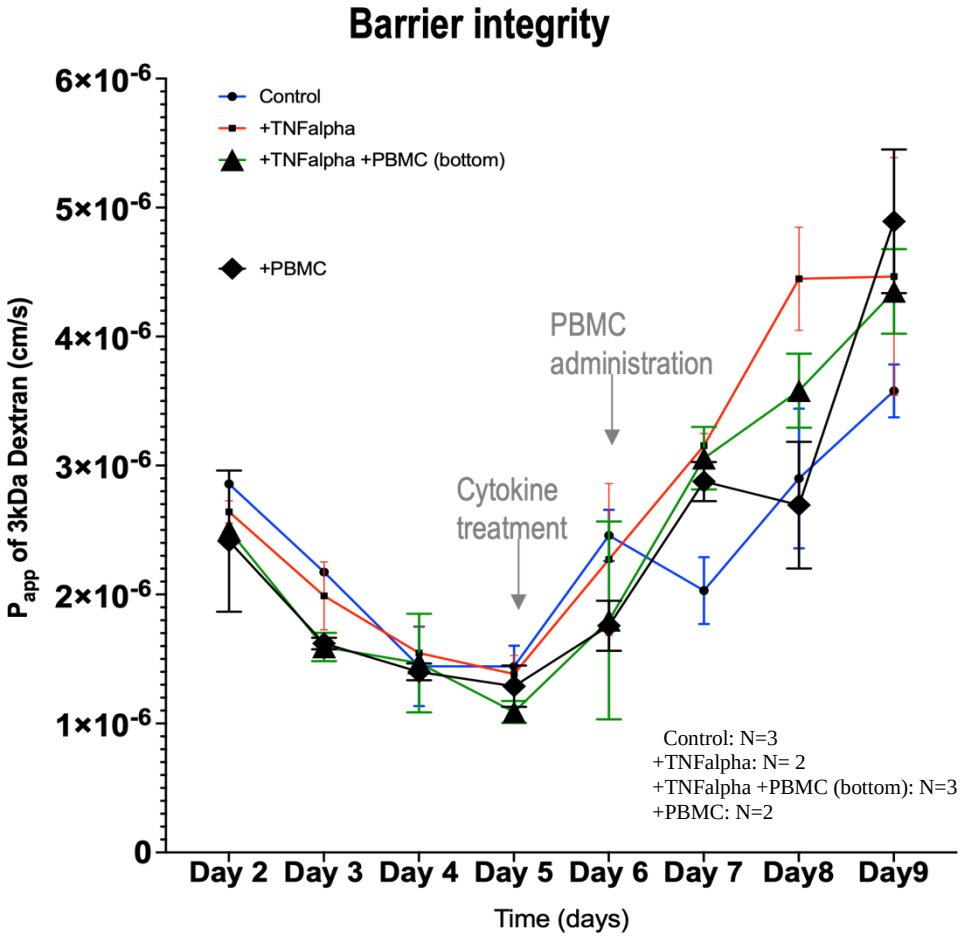

Figure 15. Analysis of 3kDa Dextran permeability assay reveals increased intestinal barrier permeability in the Presence of TNF-a.

4.2.2 Verifying PBMC activation

Increased secretion of IL-22 and IFN-γ was observed through ELISA in the effluents of chips that were exposed to primed PBMCs (**Figure 16**). This

result confirms the activation of PBMCs after priming and hints at the initiation of an inflammatory response in the intestine.

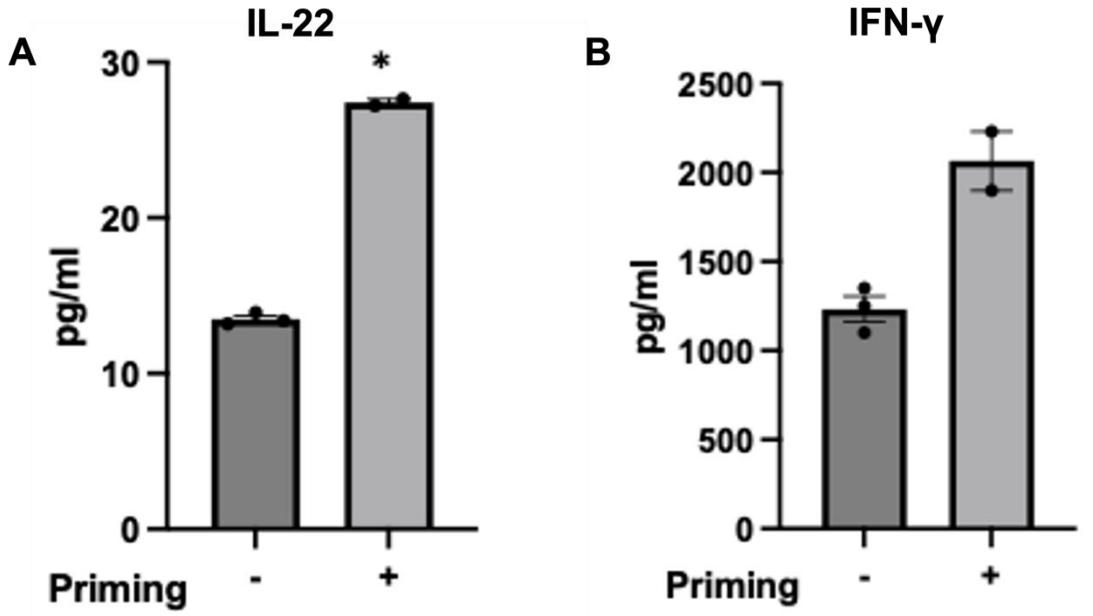

Figure 16. Increased levels of IL-22 and IFN-γ in chip effluents after exposure to primed PBMCs. (A) ELISA for the detection of IL-22. (B) ELISA for the detection of IFN-γ.

4.3 Establishment of CRC organoids

CRC lines, with distinct genetic mutation profiles were commercially purchased (**Table 1.**) When each line was thawed and put in Matrigel drops to grow, we observed different phenotypic characteristics and proliferation of the organoids. Given the identical culture conditions, these findings suggest that the difference in the growth patterns might be associated with the different underlying genetics of the organoids (**Figure 17**).

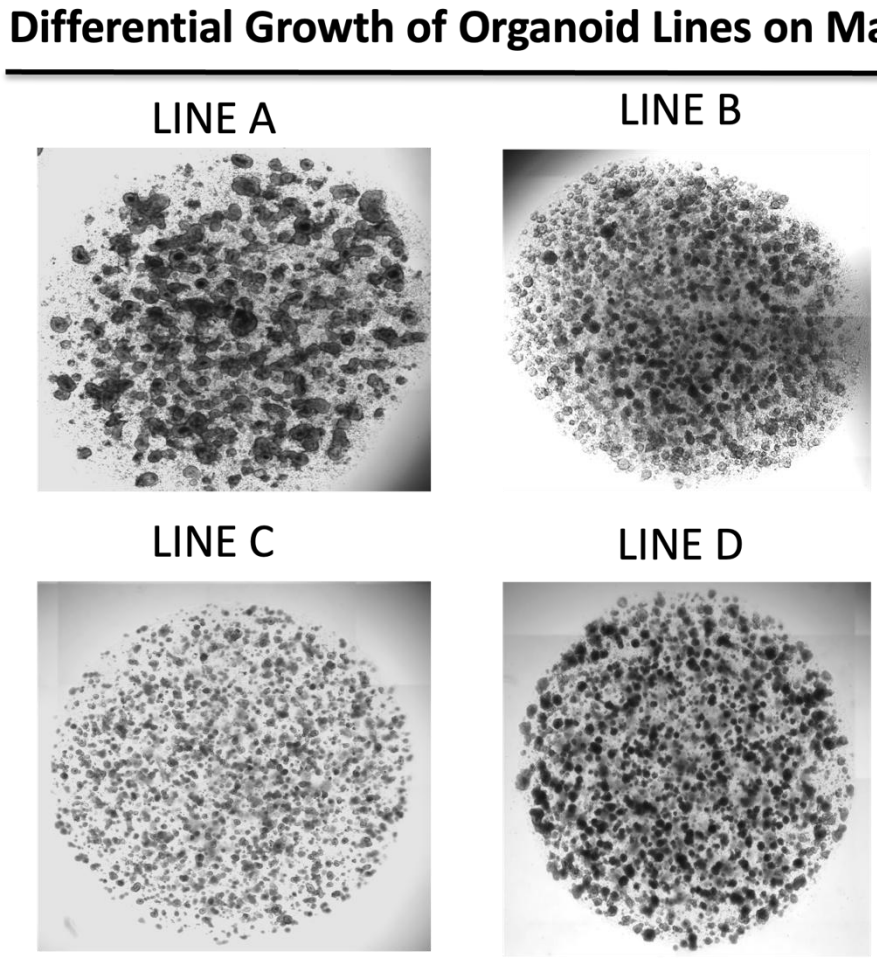

Figure 17. Bright field image of thawed CRC organoids at day 7.

4.4 Establishment and evaluation of CRC-on-a-Chip

Tumor organoids can model the intertumoral heterogeneity that is present in vivo tumors, and thus they represent a promising model to study the disease and apply novel therapeutics. As mentioned in Materials and methods, we established CRC on chip (**Figure 18**), measured the barrier integrity of each chip, as mentioned above, and treated some of the chips with Interferon-γ to examine its effect on the intestinal epithelial barrier. Surprisingly, we did not observe any changes in barrier integrity, suggesting that may be CRC organoids are resistant to inflammatory conditions especially since the majority of CRC tumors is considered immunologically cold [77].

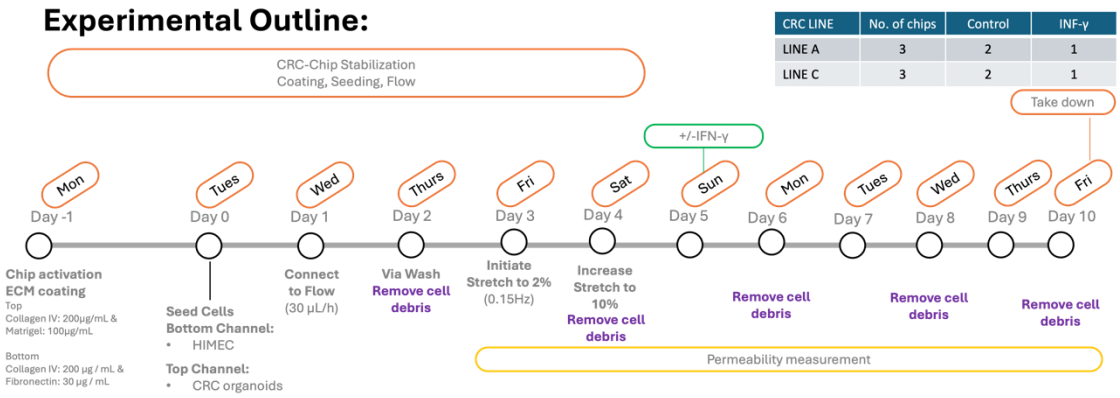

Figure 18. Outline of the CRC-on-chip establishment.

The established CRC chips were morphologically which were morphologically different from those derived from normal colon organoids, while at the same time different morphology was displayed across different CRC lines, signifying the effect of their mutational background towards their respective phenotypes (**Figure 19**). Organoid lines A and C were chosen to be stained, since they were the lines with the lowest and the greatest number of mutations respectively. The chips were fixed and stained for the cell nuclei (Hoechst), VE-Cadherin and ZO-1. Using a Zeiss LSM 880 Confocal Microscope, the formation of CRC tissues on chips and the expression of ZO-1 and E-Cadherin was observed.

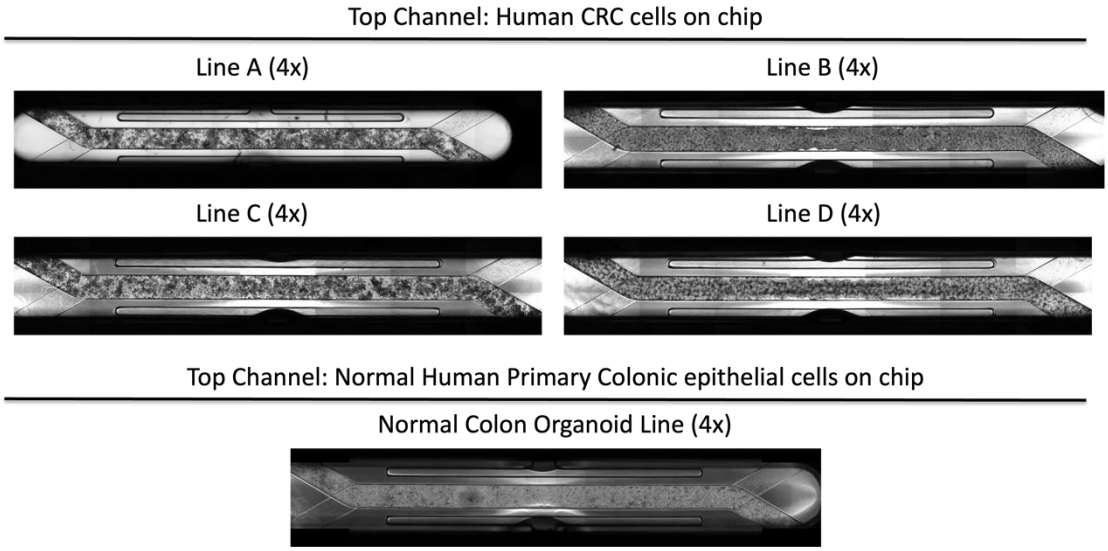

Figure 19. Representative bright field pictures of established Organoids-on-Chip systems.

CRC organoids of line A were successfully seeded on the top channel of the chip and ZO-1 (red) was detected throughout the channel (**Figure 20**), but the network of tight junctions was not as developed or organized as in the normal colon-on-chip. Additionally, E-cadherin appears to be present throughout the channel as well, indicating that the CRC cells have not undergone EMT yet and thus they have a low metastatic potential. Also, the overall cohesiveness

of CRC cells on the chips is severely lower than what was observed in the Colon chips, with plenty of gaps being present throughout the channel.

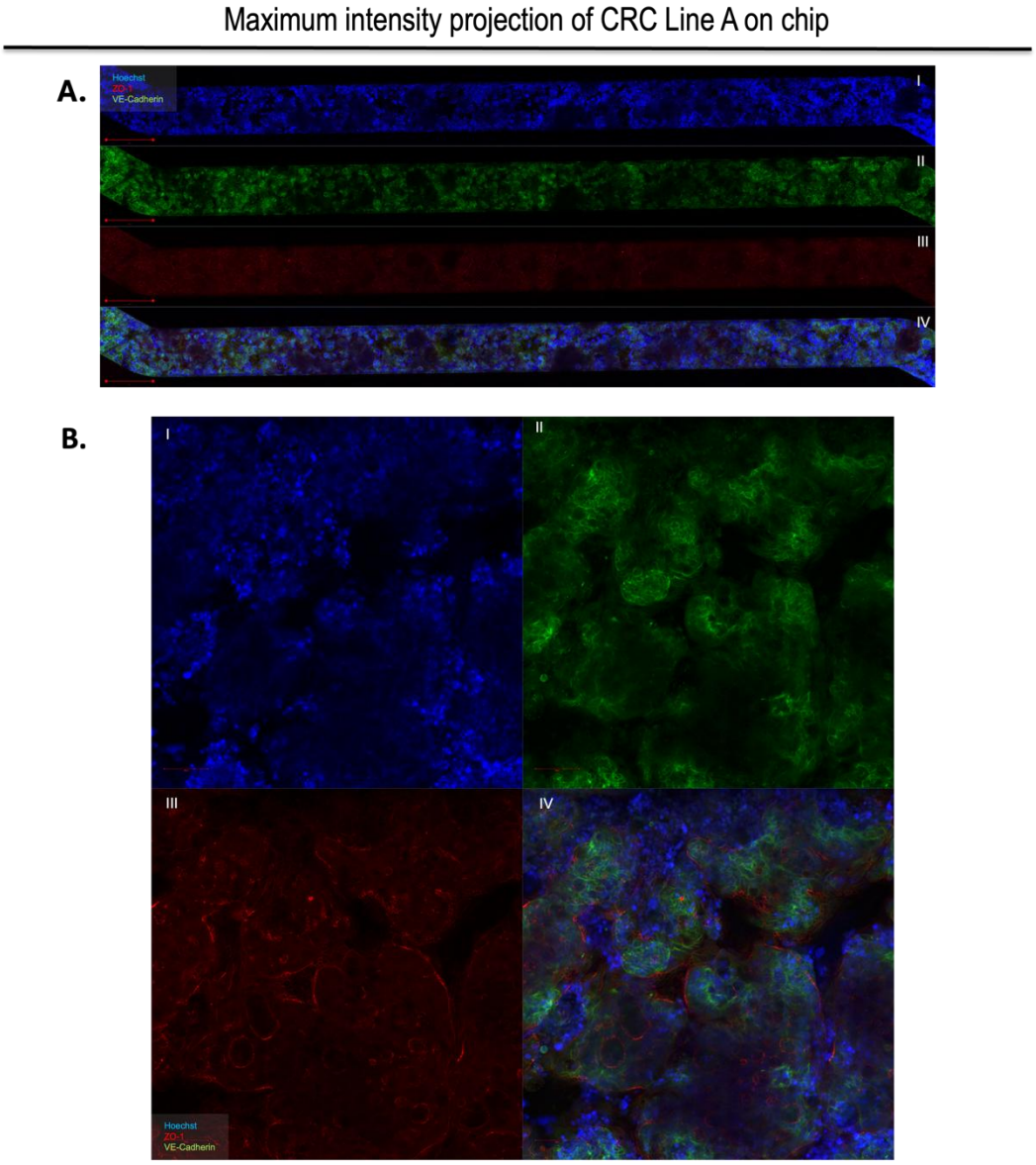

Figure 20. Representative Maximum intensity projection pictures of CRC Line A established on a chip. (A) Tile scan of chip with Line A CRC Organoids. (I) Hoechst staining, (II) E-cadherin staining, (III) ZO-1 staining and (IV) composite image. (B) Representative maximum intensity projection picture of Line A CRC organoids on the chip. (I) Hoechst staining, (II) E-cadherin staining, (III) ZO-1 staining and (IV) composite image.

1. Line A (+ IFN-γ)

CRC organoids of line A were successfully seeded on the top channel, stained for the same markers as Chip 6, with the only difference being the supplement of 30 nmol/L of IFN-γ along with the CRC medium , recreating an inflammatory microenvironment. The latter is known to have a significant effect in shaping both tumorigenesis and the plasticity of cancer cells in the

colon [78]. No significant effect on ZO-1 staining can be observed. A lower overall cohesiveness of the CRC cells in the channel, compared to its control, could be a stochastic event of unknown significance. Overall, the presence of the proinflammatory cytokine did not seem to affect the formation of the tissue on the chip (**Figure 21**).

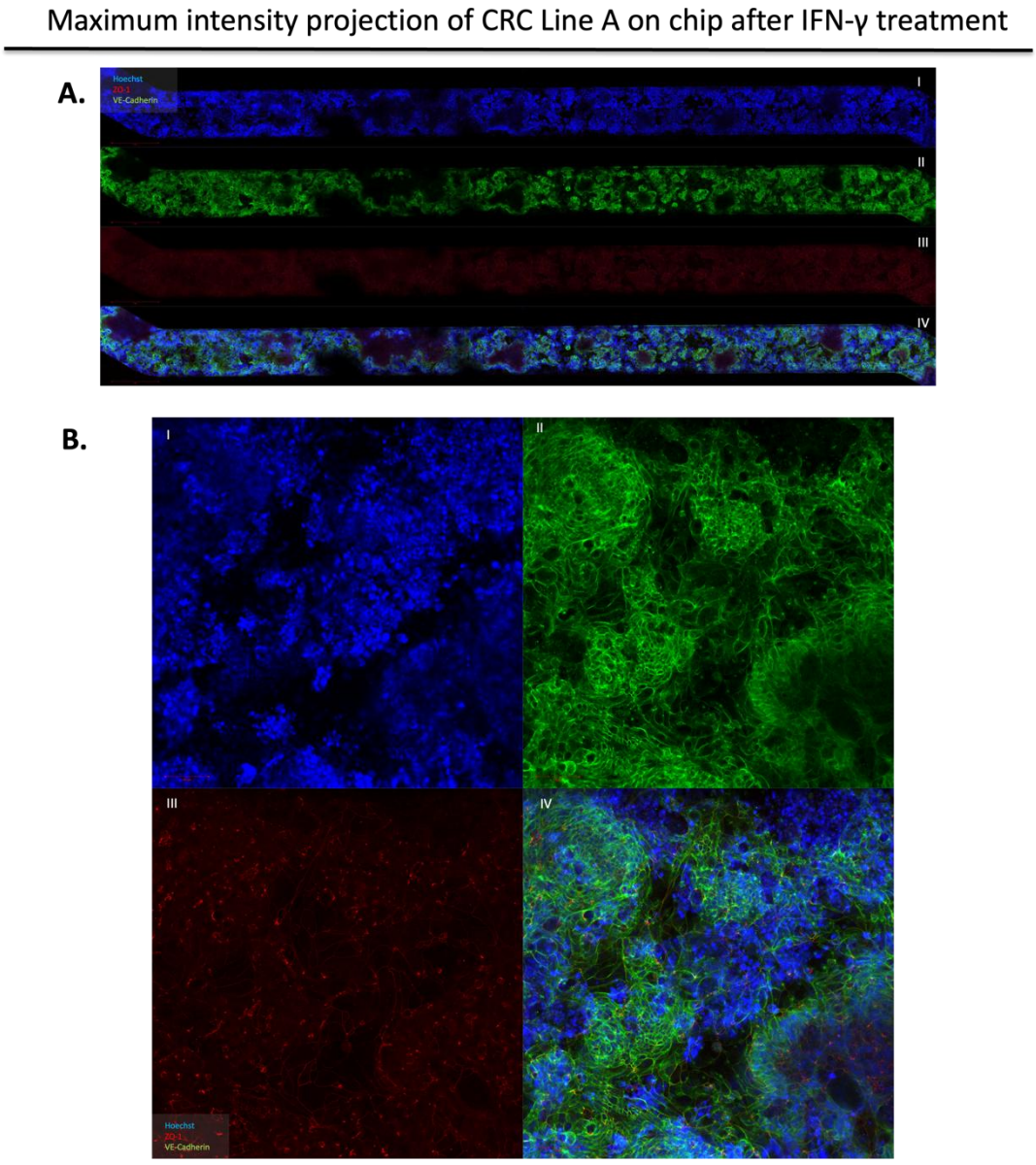

Figure 21. Representative Maximum intensity projection pictures of CRC Line A established on a chip with 100ng/ml IFN-γ treatment. No significant effect on the tight-juctions integrity was observed. (A) Tile scan of chip with Line A CRC Organoids. (I) Hoechst staining, (II) E-cadherin staining, (III) ZO-1 staining and (IV) composite image. (B) Representative maximum intensity projection picture of Line A CRC organoids on the chip. (I) Hoechst staining, (II) E-cadherin staining, (III) ZO-1 staining and (IV) composite image.

2. Line C (Control)

CRC organoids of line C were successfully seeded on the top channel and it was stained for the same markers (**Figure 22**). Organoids engrafted to the chip had a different mutational background and thus a different tissue morphology can be observed, with less cohesiveness and a more disorganized structure. Additionally, and increased expression of ZO-1 is observed, while at the same time E-cadherin seems to be slightly downregulated in comparison to the line A chips, potentially due to the high mutational burden of this organoid line and a potentially advanced epithelial–mesenchymal transition (EMT).

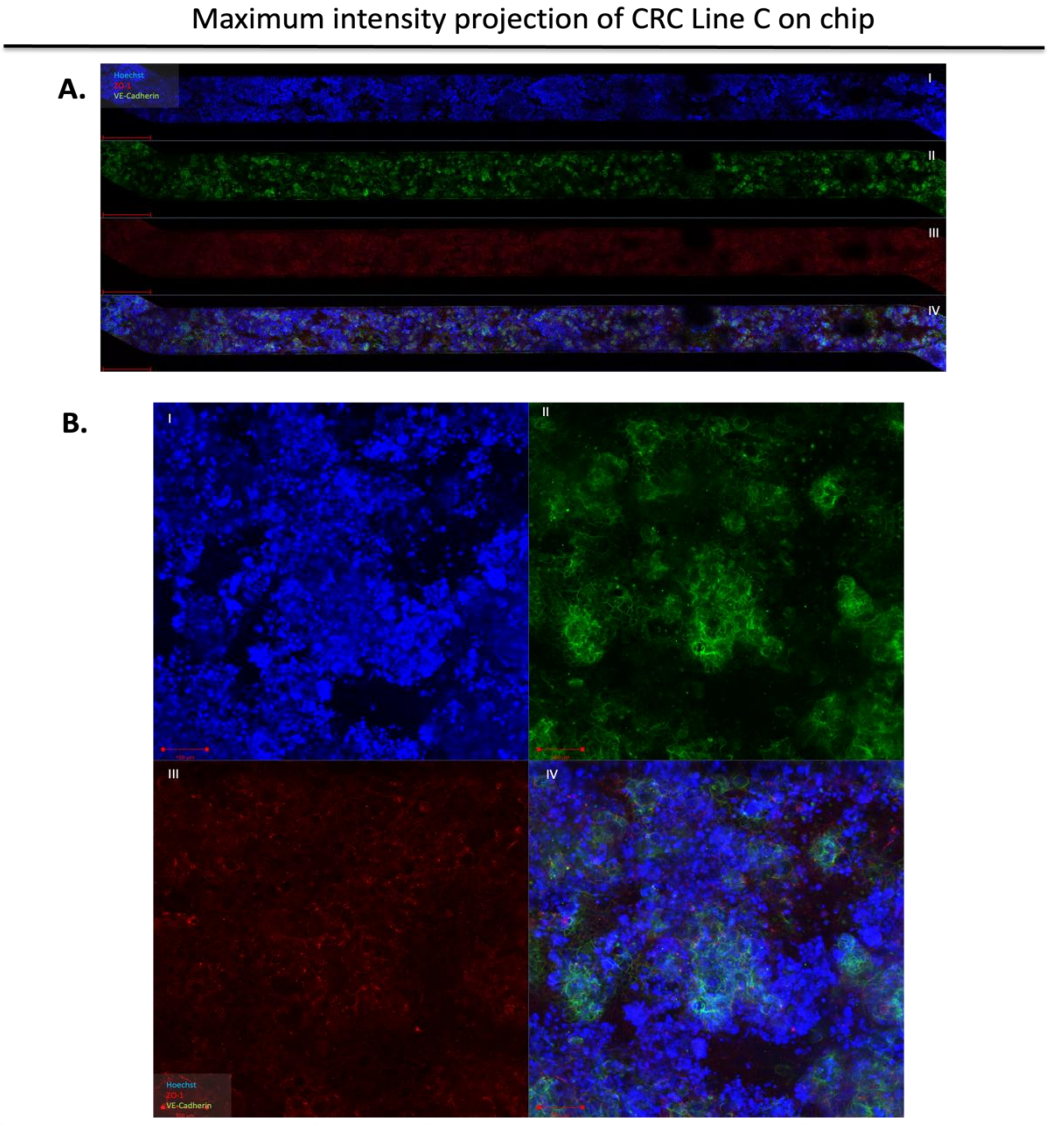

Figure 22. Representative Maximum intensity projection pictures of CRC Line C established on a chip. Reduced E-Cadherin staining is observed, pointing to a more progressed type of CRC with increased EMT and metastatic potential (A) Tile scan of chip with Line A CRC Organoids. (I) Hoechst staining, (II) E-cadherin staining, (III) ZO-1 staining and (IV) composite image. (B) Representative maximum intensity projection picture of Line A CRC organoids on the chip. (I) Hoechst staining, (II) E-cadherin staining, (III) ZO-1 staining and (IV) composite image.

3. Line C (+ IFN-γ)

CRC organoids of line C were once again successfully seeded on the top channel, but in the presence of IFN-γ (**Figure 23**). There are no major differences between the two chips from line C and thus the effect of inflammation by itself, without the addition of immune cell types, doesn't seem to have a significant effect in the biology of CRC, which is plausible due to CRC being generally considered an immunologically cold tumor.

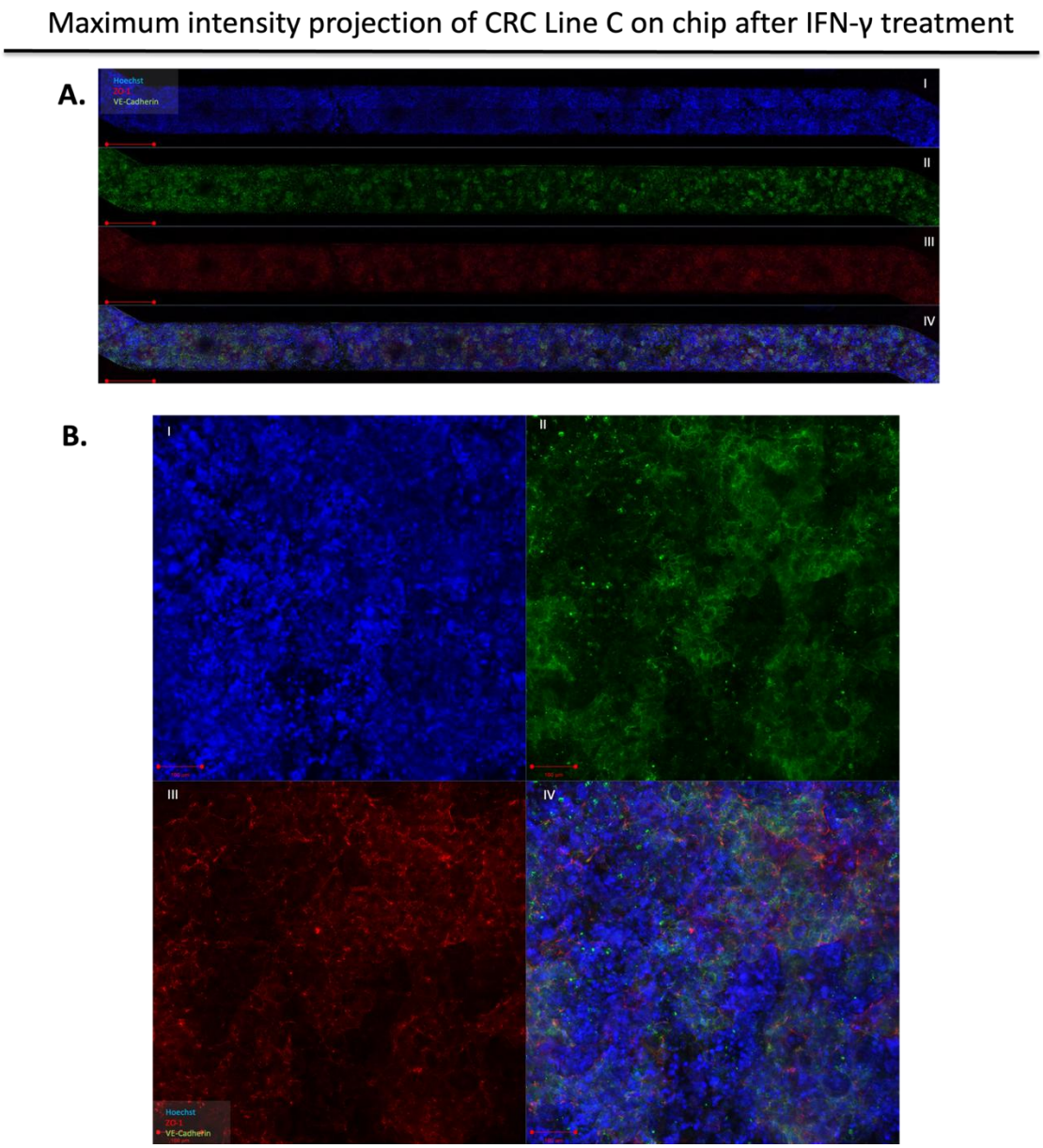

Figure 23. Representative Maximum intensity projection pictures of CRC Line C established on a chip with 100ng/ml IFN-γ treatment. (A) Tile scan of chip with Line A CRC Organoids. (I) Hoechst staining, (II) E-cadherin staining, (III) ZO-1 staining and (IV) composite image. (B) Representative maximum intensity projection picture of Line A CRC organoids on the chip. (I) Hoechst staining, (II) E-cadherin staining, (III) ZO-1 staining and (IV) composite image.

4.4.1 Resistance of CRC lines to intestinal barrier disruption

The analysis of effluents from chips seeded with CRC organoids using the 3kDa Dextran permeability assay (**Figure 24**) confirmed that IFN-γ has no significant effect in the permeability of the intestinal barrier. Therefore, the integrity of the intestinal barrier appears to be resistant to proinflammatory cytokines in CRC tissues. It's also worth noting that chips with CRC lines B and D are characterized by a less permeable barrier than lines A and C, in which several gaps can be observed throughout their tissues (**Figure 19**). Additionally, chips with CRC lines A and B display a modest increase permeability when treated with IFN-γ, which could hint to a differential resistance to inflammation between each line, although this change is nowhere near the levels observed on the healthy colon chips (**Figure 10**).

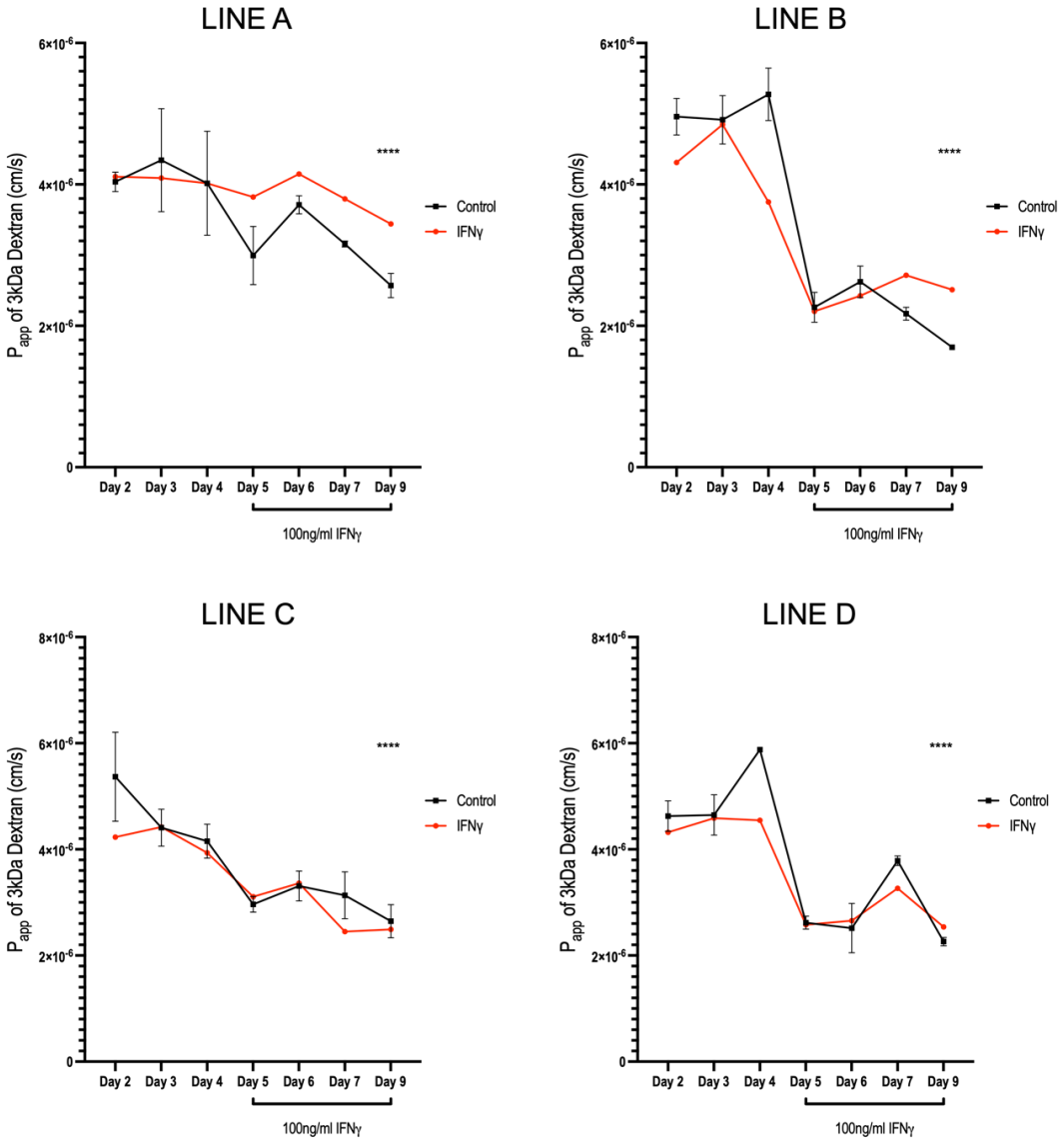

Figure 24. IFN-γ treatment has no effect in the integrity of the intestinal barrier.

5. Summary

The human intestine is a key organ for systemic homeostasis, with a well characterized structure, dynamic microenvironment and multifaceted functions. Unfortunately, it is also a site of complex serious diseases, which cannot be fully recapitulated by conventional experimental models of disease resulting in yet elusive pathologies. New approaches including human organoids cultured in microphysiological Organ-Chip platforms, aim to create an in vitro model of organs to emulate healthy and diseased states. Unlike animal models and 2D cell cultures, these alternatives offer great potential on recreating the effects of a human microenvironment to a tissue, but also to accurately recapitulate aspects of human physiology and mechanistic aspects in human disease. However, organoids and organs-on-chips also bear significant disadvantages, like high production costs, tedious maintenance, necessity of expertise, high variability and lack of high throughput screening capabilities when combined together. Organoids on their own are also characterized by great heterogeneity and the most commonly used hydrogel matrices are made of Matrigel, the protein profile of which is largely uncharacterized.

In this study, human-derived colon and CRC organoids were cultured and then seeded on chips, in order to develop models of intestinal diseases, that could provide insights to human tissue biology or be used in preclinical /translational studies as a supporting human in vitro model with physiologically relevant responses. Firstly, a human organoid-derived colon was successfully recreated on a chip in house, with a mature intestinal barrier and the presence of both endothelial and epithelial intestinal cells, with the latter differentiating into different epithelial cell subtypes present in vivo in the intestinal epithelium as previously published. This model was used to evaluate the effect of inflammation on the intestinal barrier integrity, and indeed the epithelial barrier was significantly disrupted when exposed to IFN-γ, recreating a significant hallmark of chronic inflammatory intestinal diseases on an in vitro microphysiological system. We used this colon-chip model to recreate the migration of PBMCs from the endothelial to the epithelial surface of the intestine in the context of tissue inflammation, such as in cancer, IBD and other pathologies as published before. This model would be used to test immune cell-dependent therapeutic proteins in development for the treatment of CRC. Subsequently, a CRC-Chip model was designed using patient derived CRC organoids with distinct genetic mutation backgrounds. These models showed an altered tissue morphology and tight-junctions network compared to the regular colon-chips, while at the same time they remained unaffected in an inflammatory setting, possibly due to the immunologically protected, “cold”, profile of most CRCs. Similar organoid-chip models have been previously designed and published. However the goal of this thesis was to design and validate them in-house, in order to confirm their reproducibility and robustness, and potentially use them as a companion to already existing models, for the investigation of therapeutic targets and the evaluation of novel therapeutics at a preclinical, human cell-based level.

Thus, this study underscores the potential of in vitro microphysiological systems in recreating complex biological systems that possess an accurate representation of an in vivo microenvironment with increased clinical relevance and even including distinct genetic backgrounds. These models would provide new insights on the molecular mechanisms underlying disease pathogenesis and mechanisms underlying the differences in responses to pharmacological interventions.

References

1. Lancaster MA, Knoblich JA. Organogenesis in a dish: Modeling development and disease using organoid technologies. Science (1979). 2014;345.
2. Sayed IM, El-Hafeez AAA, Maity PP, Das S, Ghosh P. Modeling colorectal cancers using multidimensional organoids. 2021. p. 345–83.
3. Chung CY, Iida-Klein A, Wyatt LE, Rudkin GH, Ishida K, Yamaguchi DT, et al. Serial Passage of MC3T3-E1 Cells Alters Osteoblastic Function and Responsiveness to Transforming Growth Factor-β1 and Bone Morphogenetic Protein-2. Biochem Biophys Res Commun. 1999;265:246–51.
4. Breslin S, O'Driscoll L. Three-dimensional cell culture: the missing link in drug discovery. Drug Discov Today. 2013;18:240–9.
5. Junttila MR, de Sauvage FJ. Influence of tumour micro-environment heterogeneity on therapeutic response. Nature. 2013;501:346–54.
6. Porter RJ, Murray GI, McLean MH. Current concepts in tumour-derived organoids. Br J Cancer. 2020;123:1209–18.
7. Mak IW, Evaniew N, Ghert M. Lost in translation: animal models and clinical trials in cancer treatment. Am J Transl Res. 2014;6:114–8.
8. Jang K-J, Otieno MA, Ronxhi J, Lim H-K, Ewart L, Kodella KR, et al. Reproducing human and cross-species drug toxicities using a Liver-Chip. Sci Transl Med. 2019;11.
9. Hofer M, Lutolf MP. Engineering organoids. Nat Rev Mater. 2021;6:402–20.
10. Zhao Z, Chen X, Dowbaj AM, Sljukic A, Bratlie K, Lin L, et al. Organoids. Nature Reviews Methods Primers. 2022;2:94.
11. Sato T, Vries RG, Snippert HJ, van de Wetering M, Barker N, Stange DE, et al. Single Lgr5 stem cells build crypt-villus structures in vitro without a mesenchymal niche. Nature. 2009;459:262–5.
12. Azar J, Bahmad HF, Daher D, Moubarak MM, Hadadeh O, Monzer A, et al. The Use of Stem Cell-Derived Organoids in Disease Modeling: An Update. Int J Mol Sci. 2021;22:7667.
13. Ashok A, Choudhury D, Fang Y, Hunziker W. Towards manufacturing of human organoids. Biotechnol Adv. 2020;39:107460.
14. Aisenbrey EA, Murphy WL. Synthetic alternatives to Matrigel. Nat Rev Mater. 2020;5:539–51.
15. Orkin RW, Gehron P, McGoodwin EB, Martin GR, Valentine T, Swarm R. A murine tumor producing a matrix of basement membrane. J Exp Med. 1977;145:204–20.
16. Kleinman HK, Martin GR. Matrigel: Basement membrane matrix with biological activity. Semin Cancer Biol. 2005;15:378–86.
17. Günther C, Winner B, Neurath MF, Stappenbeck TS. Organoids in gastrointestinal diseases: from experimental models to clinical translation. Gut. 2022;71:1892–908.

18. Kavand H, Nasiri R, Herland A. Advanced Materials and Sensors for Microphysiological Systems: Focus on Electronic and Electrooptical Interfaces. Advanced Materials. 2022;34.
19. Wang Y, Gunasekara DB, Reed MI, DiSalvo M, Bultman SJ, Sims CE, et al. A microengineered collagen scaffold for generating a polarized crypt-villus architecture of human small intestinal epithelium. Biomaterials. 2017;128:44–55.
20. Clevers H. Modeling Development and Disease with Organoids. Cell. 2016;165:1586–97.
21. Teriyapirom I, Batista-Rocha AS, Koo B-K. Genetic engineering in organoids. J Mol Med. 2021;99:555–68.
22. Vlachogiannis G, Hedayat S, Vatsiou A, Jamin Y, Fernández-Mateos J, Khan K, et al. Patient-derived organoids model treatment response of metastatic gastrointestinal cancers. Science (1979). 2018;359:920–6.
23. Kathuria A, Lopez-Lengowski K, Watmuff B, Karmacharya R. Comparative Transcriptomic Analysis of Cerebral Organoids and Cortical Neuron Cultures Derived from Human Induced Pluripotent Stem Cells. Stem Cells Dev. 2020;29:1370–81.
24. Wang H-M, Zhang C-Y, Peng K-C, Chen Z-X, Su J-W, Li Y-F, et al. Using patient-derived organoids to predict locally advanced or metastatic lung cancer tumor response: A real-world study. Cell Rep Med. 2023;4:100911.
25. Sato T, Clevers H. Growing Self-Organizing Mini-Guts from a Single Intestinal Stem Cell: Mechanism and Applications. Science (1979). 2013;340:1190–4.
26. Huch M, Gehart H, van Boxtel R, Hamer K, Blokzijl F, Verstegen MMA, et al. Long-Term Culture of Genome-Stable Bipotent Stem Cells from Adult Human Liver. Cell. 2015;160:299–312.
27. Ma B, Leijten JCH, Wu L, Kip M, van Blitterswijk CA, Post JN, et al. Gene expression profiling of dedifferentiated human articular chondrocytes in monolayer culture. Osteoarthritis Cartilage. 2013;21:599–603.
28. de Poel E, Lefferts JW, Beekman JM. Intestinal organoids for Cystic Fibrosis research. Journal of Cystic Fibrosis. 2020;19:S60–4.
29. Sugimoto S, Ohta Y, Fujii M, Matano M, Shimokawa M, Nanki K, et al. Reconstruction of the Human Colon Epithelium In Vivo. Cell Stem Cell. 2018;22:171-176.e5.
30. Yui S, Nakamura T, Sato T, Nemoto Y, Mizutani T, Zheng X, et al. Functional engraftment of colon epithelium expanded in vitro from a single adult Lgr5+ stem cell. Nat Med. 2012;18:618–23.
31. Fordham RP, Yui S, Hannan NRF, Soendergaard C, Madgwick A, Schweiger PJ, et al. Transplantation of Expanded Fetal Intestinal Progenitors Contributes to Colon Regeneration after Injury. Cell Stem Cell. 2013;13:734–44.
32. Vuorenpää H, Björninen M, Välimäki H, Ahola A, Kroon M, Honkamäki L, et al. Building blocks of microphysiological system to model physiology and pathophysiology of human heart. Front Physiol. 2023;14.
33. Bhatia SN, Ingber DE. Microfluidic organs-on-chips. Nat Biotechnol. 2014;32:760–72.
34. Kaji I, Thiagarajah JR, Goldenring JR. Modeling the cell biology of monogenetic intestinal epithelial disorders. Journal of Cell Biology. 2024;223.

35. Zhang B, Korolj A, Lai BFL, Radisic M. Advances in organ-on-a-chip engineering. Nat Rev Mater. 2018;3:257–78.
36. Huh D, Matthews BD, Mammoto A, Montoya-Zavala M, Hsin HY, Ingber DE. Reconstituting Organ-Level Lung Functions on a Chip. Science (1979). 2010;328:1662–8.
37. Esch EW, Bahinski A, Huh D. Organs-on-chips at the frontiers of drug discovery. Nat Rev Drug Discov. 2015;14:248–60.
38. Park S-H, Sim WY, Min B-H, Yang SS, Khademhosseini A, Kaplan DL. Chip-Based Comparison of the Osteogenesis of Human Bone Marrow- and Adipose Tissue-Derived Mesenchymal Stem Cells under Mechanical Stimulation. PLoS One. 2012;7:e46689.
39. Radisic M, Park H, Shing H, Consi T, Schoen FJ, Langer R, et al. Functional assembly of engineered myocardium by electrical stimulation of cardiac myocytes cultured on scaffolds. Proceedings of the National Academy of Sciences. 2004;101:18129–34.
40. Wang Y, Qin J. Advances in human organoids-on-chips in biomedical research. Life Medicine. 2023;2.
41. Tang X-Y, Wu S, Wang D, Chu C, Hong Y, Tao M, et al. Human organoids in basic research and clinical applications. Signal Transduct Target Ther. 2022;7:168.
42. Homan KA, Gupta N, Kroll KT, Kolesky DB, Skylar-Scott M, Miyoshi T, et al. Flow-enhanced vascularization and maturation of kidney organoids in vitro. Nat Methods. 2019;16:255–62.
43. Wang Y, Wang L, Guo Y, Zhu Y, Qin J. Engineering stem cell-derived 3D brain organoids in a perfusable organ-on-a-chip system. RSC Adv. 2018;8:1677–85.
44. Kasendra M, Tovaglieri A, Sontheimer-Phelps A, Jalili-Firoozinezhad S, Bein A, Chalkiadaki A, et al. Development of a primary human Small Intestine-on-a-Chip using biopsy-derived organoids. Sci Rep. 2018;8:2871.
45. Yin F, Zhang X, Wang L, Wang Y, Zhu Y, Li Z, et al. HiPSC-derived multi-organoids-on-chip system for safety assessment of antidepressant drugs. Lab Chip. 2021;21:571–81.
46. Dekker E, Tanis PJ, Vleugels JLA, Kasi PM, Wallace MB. Colorectal cancer. The Lancet. 2019;394:1467–80.
47. Li J, Ma X, Chakravarti D, Shalapour S, DePinho RA. Genetic and biological hallmarks of colorectal cancer. Genes Dev. 2021;35:787–820.
48. Bray F, Ferlay J, Soerjomataram I, Siegel RL, Torre LA, Jemal A. Global cancer statistics 2018: GLOBOCAN estimates of incidence and mortality worldwide for 36 cancers in 185 countries. CA Cancer J Clin. 2018;68:394–424.
49. Jess T, Rungoe C, Peyrin–Biroulet L. Risk of Colorectal Cancer in Patients With Ulcerative Colitis: A Meta-analysis of Population-Based Cohort Studies. Clinical Gastroenterology and Hepatology. 2012;10:639–45.
50. Ullman TA, Itzkowitz SH. Intestinal Inflammation and Cancer. Gastroenterology. 2011;140:1807-1816.e1.
51. Shin AE, Giancotti FG, Rustgi AK. Metastatic colorectal cancer: mechanisms and emerging therapeutics. Trends Pharmacol Sci. 2023;44:222–36.

52. Fumagalli A, Oost KC, Kester L, Morgner J, Bornes L, Bruens L, et al. Plasticity of Lgr5-Negative Cancer Cells Drives Metastasis in Colorectal Cancer. Cell Stem Cell. 2020;26:569-578.e7.
53. Barker N, van Es JH, Kuipers J, Kujala P, van den Born M, Cozijnsen M, et al. Identification of stem cells in small intestine and colon by marker gene Lgr5. Nature. 2007;449:1003–7.
54. Batlle E, Clevers H. Cancer stem cells revisited. Nat Med. 2017;23:1124–34.
55. Cañellas-Socias A, Cortina C, Hernando-Momblona X, Palomo-Ponce S, Mulholland EJ, Turon G, et al. Metastatic recurrence in colorectal cancer arises from residual EMP1+ cells. Nature. 2022;611:603–13.
56. Aiello NM, Maddipati R, Norgard RJ, Balli D, Li J, Yuan S, et al. EMT Subtype Influences Epithelial Plasticity and Mode of Cell Migration. Dev Cell. 2018;45:681-695.e4.
57. Richmond CA, Shah MS, Carlone DL, Breault DT. An enduring role for quiescent stem cells. Developmental Dynamics. 2016;245:718–26.
58. Powrie F, Uhlig H. Animal models of intestinal inflammation: clues to the pathogenesis of inflammatory bowel disease. Novartis Found Symp. 2004;263:164–74; discussion 174-8, 211–8.
59. Iliopoulou L, Kollias G. Harnessing murine models of Crohn's disease ileitis to advance concepts of pathophysiology and treatment. Mucosal Immunol. 2022;15:10–26.
60. Pothuraju R, Khan I, Jain M, Bouvet M, Malafa M, Roy HK, et al. Colorectal cancer murine models: Initiation to metastasis. Cancer Lett. 2024;587:216704.
61. Artursson P. Epithelial Transport Of Drugs In Cell Culture. I: A Model For Studying The Passive Diffusion Of Drugs Over Intestinal Absorbtive (Caco-2) Cells. J Pharm Sci. 1990;79:476–82.
62. Dahlgren D, Sjöblom M, Lennernäs H. Intestinal absorption-modifying excipients: A current update on preclinical in vivo evaluations. European Journal of Pharmaceutics and Biopharmaceutics. 2019;142:411–20.
63. Kasendra M, Luc R, Yin J, Manatakis D V, Kulkarni G, Lucchesi C, et al. Duodenum Intestine-Chip for preclinical drug assessment in a human relevant model. Elife. 2020;9.
64. Pimenta J, Ribeiro R, Almeida R, Costa PF, da Silva MA, Pereira B. Organ-on-Chip Approaches for Intestinal 3D In Vitro Modeling. Cell Mol Gastroenterol Hepatol. 2022;13:351–67.
65. Yu H, Hasan NM, In JG, Estes MK, Kovbasnjuk O, Zachos NC, et al. The Contributions of Human Mini-Intestines to the Study of Intestinal Physiology and Pathophysiology. Annu Rev Physiol. 2017;79:291–312.
66. Gleeson JP, Estrada HQ, Yamashita M, Svendsen CN, Targan SR, Barrett RJ. Development of Physiologically Responsive Human iPSC-Derived Intestinal Epithelium to Study Barrier Dysfunction in IBD. Int J Mol Sci. 2020;21:1438.
67. Jelinsky SA, Derksen M, Bauman E, Verissimo CS, van Dooremalen WTM, Roos JL, et al. Molecular and Functional Characterization of Human Intestinal Organoids and Monolayers for Modeling Epithelial Barrier. Inflamm Bowel Dis. 2023;29:195–206.

68. Wright CW, Li N, Shaffer L, Hill A, Boyer N, Alves SE, et al. Establishment of a 96-well transwell system using primary human gut organoids to capture multiple quantitative pathway readouts. Sci Rep. 2023;13:16357.
69. Kim HJ, Huh D, Hamilton G, Ingber DE. Human gut-on-a-chip inhabited by microbial flora that experiences intestinal peristalsis-like motions and flow. Lab Chip. 2012;12:2165.
70. Grassart A, Malardé V, Gobaa S, Sartori-Rupp A, Kerns J, Karalis K, et al. Bioengineered Human Organ-on-Chip Reveals Intestinal Microenvironment and Mechanical Forces Impacting Shigella Infection. Cell Host Microbe. 2019;26:435-444.e4.
71. Kasendra M, Luc R, Yin J, Manatakis D V, Kulkarni G, Lucchesi C, et al. Duodenum Intestine-Chip for preclinical drug assessment in a human relevant model. Elife. 2020;9.
72. Apostolou A, Panchakshari RA, Banerjee A, Manatakis D V., Paraskevopoulou MD, Luc R, et al. A Novel Microphysiological Colon Platform to Decipher Mechanisms Driving Human Intestinal Permeability. Cell Mol Gastroenterol Hepatol. 2021;12:1719–41.
73. Strelez C, Chilakala S, Ghaffarian K, Lau R, Spiller E, Ung N, et al. Human colorectal cancer-on-chip model to study the microenvironmental influence on early metastatic spread. iScience. 2021;24:102509.
74. Strelez C, Perez R, Chlystek JS, Cherry C, Yoon AY, Haliday B, et al. Integration of Patient-Derived Organoids and Organ-on-Chip Systems: Investigating Colorectal Cancer Invasion within the Mechanical and GABAergic Tumor Microenvironment. bioRxiv. 2023;
75. Ma TY, Iwamoto GK, Hoa NT, Akotia V, Pedram A, Boivin MA, et al. TNF-α-induced increase in intestinal epithelial tight junction permeability requires NF-κB activation. American Journal of Physiology-Gastrointestinal and Liver Physiology. 2004;286:G367–76.
76. Zhang Y, Zhao S-X, Nie L, Shen L-J, Han W. Hyperosmolarity disrupts tight junction via TNF-α/MMP pathway in primary human corneal epithelial cells. Int J Ophthalmol. 2022;15:683–9.
77. Ma S-X, Li L, Cai H, Guo T-K, Zhang L-S. Therapeutic challenge for immunotherapy targeting cold colorectal cancer: A narrative review. World J Clin Oncol. 2023;14:81–8.
78. Schmitt M, Greten FR. The inflammatory pathogenesis of colorectal cancer. Nat Rev Immunol. 2021;21:653–67.